CHAPTER 6

Technology, RF, and Energy Working Group Assessments

6.1 INTRODUCTION

The charge of the Technology, RF Power, and Energy Performance Working Group is recalled here:

> "This group will play a role similar to the first ILC-TRC Linac Technology working group, but will broaden its scope to analyze all those factors which affect the energy performance of all four machines. It will look at sources, injectors, magnets, cryogenics, klystrons, power supplies, modulators, rf pulse compression systems, rf amplitude and phase stability, and any other parts of the designs which determine whether the machines can reliably reach their operating energy, be tunable, and efficient in their use of electric power."

The working group has addressed the charge by subdividing its activities into five subgroups whose responsibilities are briefly described:

1. Injectors and Technology Subgroup

   Members: **H. Weise**, H. Edwards, K. Hübner, P. Logatchov, M. Ross, N. Toge

   All critical technological aspects of the machines not covered in the linac sections (Section 6.3, Section 6.4, and Section 6.5) and not directly related to luminosity performance are discussed here. It includes guns and targets, positron production as well as the hardware of damping rings and beam delivery systems. In addition the main linac beam monitors are examined in this subgroup. For the convenience of the reader, the few luminosity issues connected with the injectors, upstream from the damping rings, are also presented in the corresponding chapter (see also Chapter 7).

2. RF Power Sources Subgroup

   Members: **Y.H. Chin**, H.H. Braun, L. Lilje, P. Logatchov, R. Pasquinelli, T. Shintake

   This subgroup covered the klystrons, modulators, and associated power supplies for the main linacs, and in the case of CLIC, for the drive beam linacs. In addition the main linacs low-level rf systems are discussed in this section.

3. RF Power Distribution Subgroup

   Members: **K. Hübner**, H.H. Braun, Y.H. Chin, L. Lilje, R. Pasquinelli, M. Ross, T. Shintake, P. Wilson

   This subgroup dealt with the transfer of rf power from the klystrons to the main linac accelerator structures. It covered the waveguide architecture and associated rf power components. This obviously included the pulse compression systems for the JLC-C and JLC-X/NLC projects. For CLIC, the drive beam system is considered as a distributed klystron and is globally discussed here. In addition, the reader will find in Section 6.4.5 a compilation of overall linac efficiencies for the four machines.

4. Accelerator Structures Subgroup

   Members: **P. Wilson**, C. Adolphsen, H.H. Braun, H. Edwards, L. Lilje, N. Toge, T. Shintake

   This subgroup looked at all aspects of the main linacs accelerator structures. Accelerating gradient and wakefield suppression (or High Order Mode damping) are obviously the most important parameters, but other aspects are also considered here, like coupler performance, mechanical and vacuum properties, and fabrication techniques. For the superconducting cavities, the cryostat design and cryoplant issues were also discussed by this subgroup.

5. Reliability Subgroup

   Members from Energy Working Group: **R. Pasquinelli**, C. Adolphsen, K. Hübner, M. Ross, T. Shintake, H. Weise

   This subgroup was common to the two original working groups, Technology, RF, and Energy and Luminosity Performance. The members of this subgroup from the Luminosity Working Group are given in Chapter 7.

   Although the reliability of individual components has been discussed to some extent in the previous sections, a more global approach has been taken in the Reliability subgroup. In particular, the implications of component reliability and machine architecture on the overall performance in terms of final machine up-time were discussed here. The Machine Protection System is also discussed by this subgroup.

   Contrary to the other sections, the global reliability findings are presented in Chapter 8 of the report, not in Chapter 6.

The Working Group has not examined those technology aspects that were already demonstrated. This was the case, for instance for the prelinacs of the JLC-X/NLC projects.

A major modification of the JLC-X/NLC main linacs was presented to the Working Group in September 2002, namely the replacement of the DLDS scheme by a SLED-II-based version. This modification was consistent with the original findings of the Working Group. Although many evaluations had already been made, especially by the Power Distribution subgroup, it was decided to evaluate the new scheme and incorporate the results in the final document. The original findings concerning the DLDS-based scheme are left in the Power Distribution section, for completeness.

In order to present the conclusions of each subchapter with a format as uniform as reasonably possible, the Working Group has defined categories of concerns applicable across all the reviewed items. Ranked in decreasing order of criticality, the Working Group distinguishes:

Show stoppers: A situation for which it is not plausible that the problem can be overcome by more R&D. In this case a radical design change is required. It is not surprising that the Working Group has not identified any show stoppers, as many experienced scientists have studied the projects in detail for many years.

Major concerns: A major concern appears when a problem is identified which could turn into a show stopper if the corresponding R&D is not successful AND this R&D is not planned, not funded or not possible at present. Hence, the Working Group strongly recommends to consider this R&D.

Concerns: A concern corresponds to either:

- A problem that has been identified and which could turn into a show stopper if R&D is not successful, BUT this R&D is foreseen (on going or planned, but not necessarily funded). Hence the group supports this R&D as important.
- An inherent negative feature which might have adverse effects on cost, operability, or maintainability.

Plausible solutions: The feasibility of the system has been demonstrated or is plausible by comparison to similar configurations. Further R&D is useful, but not mandatory for demonstrating the feasibility; it could be conducted for furthering engineering study or cost reduction.

In the conclusions of each section a recommended program of R&D is indicated together with the findings of the subgroup. The reader will find a comprehensive review of those R&D items, sorted by machine, detailed and ranked in Chapter 9. The R&D rankings that are quoted in some of the following subchapters are also defined in Chapter 9.

6.2 INJECTORS AND TECHNOLOGY

6.2.1 General Source Intensity Issues

The primary function of the positron and electron injectors is to provide a stored beam for each damping ring that meets the intensity and intensity stability specifications. In order to determine the specifications it is important to:

- Catalog beam loss mechanisms within the injector and then compute the required beam from the primary source
- Catalog the effects associated with beam intensity fluctuations, especially downstream of the electron damping ring

The latter includes the effects that beam intensity fluctuations can have on positron production. This has been done for the JLC-X/NLC injector systems and is reflected in the performance summary tables (see NLC ZDR).

There are three places in the injector system where losses greater than a few percent are expected:

- At the source, where the beam is captured into a longitudinal bucket
- At the end of the first linac section, where a bending system greatly narrows the energy acceptance
- As the beam is captured in the damping ring, if the longitudinal or transverse phase space exceeds the ring acceptance

For example, in the SLC positron source, the yield just after the first capture structure was 4 positrons per incoming electron. This yield decreased to about 2.5 e^+ per e^- after the capture region and energy cuts as was expected. However, the yield then decreased further during the transport and acceleration to the positron damping ring. Typical injection efficiency was about 70%. Overall, the system had a yield of roughly 1 captured positron in the damping ring for every electron incident on the target, which was ∼60% of what was predicted. In contrast, the polarized electron transport was much better. During typical operation roughly 72% of the charge from the gun was bunched and captured in the electron damping ring and during good periods the yield was as high as 84%. Almost all of the losses occurred in the bunchers or just downstream at relatively low beam energy. There were only a few percent losses during injection into the damping ring.

The losses in the SLC were not nearly as severe as they would be in a future linear collider because the beam power in the SLC injector was only ∼1 kW. In the NLC and TESLA injectors, the beam power will be roughly 50 and 200 times higher than in the SLC. However, the location of the losses should be well known. The TESLA positron source design artificially reduces the energy acceptance in the bending section at 115 MeV with moveable collimators. In the simulations, this acceptance is matched to the damping ring (DR) acceptance. Similarly in the NLC design, the energy spectrum is collimated in a

chicane located at 80 or 250 MeV for the e^- and e^+ sources, respectively. Then both the energy spectrum and the transverse phase space are collimated at 1.98 GeV before injection into the damping rings [1].

The greatest concern is in the initial longitudinal phase space capture section, where both the modelling and the hardware systems have a poor performance record in existing machines and test facilities. Losses at the end of the linac, related to a low energy tail produced in the subharmonic bunchers, can be up to 30%. R&D is needed to develop simulation codes that are more useful than those usually used (*e.g.*, PARMELA) and to test them. It should be noted that rf gun performance is usually much better, leading to losses closer to 0%. A new simulation tool (ASTRA) was used and it showed some significant differences from PARMELA, especially with respect to the longitudinal phase space. Successful benchmarking was started and is still continuing at TTF and DESY Zeuthen (PITZ).

If large beam losses are expected, then there must be a system designed to accept them. In the case of TESLA, where the beam power captured in the ring is expected to be 250 kW, commissioning dump systems at low energy as well as at 5 GeV are needed, each at the ends of the corresponding linac sections, and capable of handling up to 25 or 30% of that power. At 5 GeV energy, this dump system is challenging because of space constraints in the tunnel.

In the TESLA design the electron beam at the end of the main linac is used for positron production. For both the electron and positron injector systems, the bunch population jitter should be propagated through the system in the simulations in order to estimate these effects. In particular, the ±5% peak-to-peak jitter of the electron beam should be reviewed with respect to positron production. While transverse wakefields in the TESLA linacs are extremely small, the wakes from the beam delivery collimators are not, and they contribute to the bunch-to-bunch position fluctuations at the IP. The importance of this effect has to be investigated as well.

The important parameters of the electron and positron sources are summarized in Table 6.1 and Table 6.2 respectively.

6.2.2 Electron Source

Linear colliders need polarized e^- sources for their operation but could take advantage of an unpolarized source for commissioning, machine studies and perhaps unpolarized luminosity operation purposes, if needed. The need for a low technical risk, reliable injector system strongly impacts the design effort. The chosen technologies are based on the experience with previously built and operated colliders like, for example, the SLC and fourth generation light sources (LCLS and TESLA-FEL). With respect to the polarized source all LC projects are planning for a dc photocathode gun very similar to the successfully operated SLC polarized source [2]. Therefore the technical risk seems low enough.

6.2.2.1 Luminosity Issues

Electron polarization of 80% is required. Polarization at the damping ring entrance is achieved by producing polarized electrons at the source and transporting them through the

TABLE 6.1
Tables for Electrons

	TESLA	NLC	CLIC
Parameters at damping ring			
Energy E_0 [GeV]	5.0	1.98	2.42
Number of particles/bunch N_p	2×10^{10}	0.8×10^{10}	0.63×10^{10}
Bunch length (FWHM) [mm]	<10	10	3
Energy spread $\Delta E/E_0$ [%]	1	1	2
Normalized RMS emittance $\gamma\varepsilon$ [μm·rad]	40	100	10
Position jitter	0.1σ	1.0σ	
Number of bunches	2820	192	154
Repetition rate [Hz]	5	120	200
Bunch spacing [ns]	337	1.4	0.666
Polarization [%]	80	80	75
Gun			
Peak current [A]	2	1	3
Bunch length [mm]	600	150	100
Number of particles/second [s^{-1}]	2.8×10^{14}	1.8×10^{14}	1.9×10^{14}
Laser pulse length [ns]	2	0.5	
Laser energy/bunch [μJ]	4.6	4.2	
Bunching system			
f_{RF1} [MHz]	108	714	1500
f_{RF2} [MHz]	433		1500
f_{RF3} [MHz]	1300 (normal conducting)		
Pre-linac			
f_{RF} [MHz]	1300 (super-conducting)	2856	1500

TABLE 6.2
Tables for Positrons

	TESLA	NLC	CLIC
Parameters at (pre) damping ring			
Energy E_0 [GeV]	5.0	1.98	2.42
Number of particles/bunch N_p	2×10^{10}	0.9×10^{10}	0.63×10^{10}
Bunch length (FWHM) [mm]	<10	15	7
Energy spread $\Delta E/E_0$ [%]	±0.8	±1.0	±2.0
Normalized edge emittance $\gamma\varepsilon$ [m·rad]	0.014	0.03	0.09
Position jitter	0.1σ	1.0σ	
Number of bunches	2820	190	154
Repetition rate [Hz]	5	120	200
Bunch spacing [ns]	337	1.4	0.666
Reachable polarization [%]	45–50	Not fully studied	Not fully studied
Incident beam			
Method	Undulator	e^- drive linac	
Incident beam energy [GeV]	250–150	6.2	2.0
Target			
Material / thickness [rad. length]	Ti / 0.4	WRe / 4	
Number of targets	1	3	1
Number of particles/second [s^{-1}]	2.8×10^{14}	2.6×10^{14}	1.9×10^{14}
Peak energy deposition [J/g]		<35	<42
Average power deposition [kW]	5		16
Positron yield			
At damping ring	2 - 1	1	0.6

subsequent buncher and linac sections. A rigorous spin tracking study for this case has not yet been performed, mainly due to the fact that no major problems are envisioned. In addition, the emittance was evaluated with the help of space charge tracking codes like PARMELA. TESLA calculates a normalized RMS emittance of 42.5 μm·rad, while JLC-X/NLC assumes 100 μm·rad based on a more conservative approach to error margins.

6.2.2.2 Choice of Technology

For the production of polarized electrons, a polarized high-power laser (typically 5 μJ per pulse, wavelength around 800 nm) illuminates a semiconductor photocathode (GaAs) placed in a high-voltage dc gun (typically 120 to 200 kV at gradients of a few MV/m). The produced polarized electron beam is then bunched by means of one or several subharmonic pre-bunching cavities, accelerated first by solenoid-focused normal-conducting accelerator sections, and finally further accelerated by either normal-conducting (CLIC and JLC/NLC) or superconducting sections (TESLA). The energy needed for the damping ring injection varies between 1.98 and 5 GeV. The main difference between the linear collider approaches is the bunch spacing (nanoseconds for JLC/NLC and CLIC, a few 100 ns for TESLA), and the number of bunches per train (CLIC: 154, JLC/NLC: 192, and TESLA: 2820–4886). Both parameters directly reflect the choice of linac technology. The bunch train length, which must be less than the rf pulse length, is below 1 μs for normal-conducting accelerator sections while for superconducting sections it is 1 ms.

6.2.2.3 Key Issues

The key issues in providing a reliably operating polarized e^- source are: ultra-high vacuum conditions (10^{-11} mbar) in the gun, low dark currents, *i.e.*, modest electric fields at the cathode, operating within the cathode charge limit which defines the maximum current density at the cathode, allowing sufficient cathode recovery time during multibunch operation, and laser technology.

The successful operation of the SLC injector qualifies the choice of technology. But because of the higher bunch train charge requirements, JLC/NLC and CLIC need improvement of the photo-cathodes with respect to the SLC cathodes. Recent results from a gradient-doped cathode are very promising: the cathode operated for roughly 6 months during the 2002 E-158 experiment at SLAC and produced roughly 5 times the charge required for the JLC/NLC design during tests. Additional studies will be aimed at developing a further optimized cathode material.

A laser very similar to the one needed for driving the TESLA polarized gun is currently under construction. This laser is being built for time resolved spectroscopy at the TTF FEL. It delivers 800 μs long trains of 10 μJ pulses at a wavelength around 800 nm in a first step separated by 1 μs [3]. The pulse length can be adjusted between 20 ps and 200 fs. This common effort of different institutes uses a Nd:YLF burst-mode laser, a weak TiSa seed-pulse oscillator and two nonlinear crystals as an optical parametric amplifier. The collaboration aims for a pump-probe facility with sub-picosecond time resolution to be used at the TTF FEL in 2004. Bigger subsystems of this new laser are going to be installed at the rf gun test facility PITZ (DESY Zeuthen) in 2002.

One important parameter in the laser specification is the amplitude or energy jitter which directly converts to an intensity jitter of the source. The intensity jitter transforms into an emittance jitter due to space charge forces and an energy jitter due to beam loading. The TESLA design assumes a bunch-to-bunch population jitter of ±5% peak-to-peak. This requirement is based on the TESLA low emittance transport calculation. The new laser has demonstrated 800 μs long trains with an energy stability at the interaction region on the order of a few percent rms which is consistent with the TESLA specifications. For the NLC the population jitter is specified to be smaller than 1% full-width for the train-to-train jitter and 2% rms for bunch-to-bunch jitter. The CLIC design requires 1% rms bunch-to-bunch population jitter and 0.5% train-to-train jitter. The resulting laser specification has not been met. Further R&D is needed for both designs.

The photoinjector option of the CLIC (3 TeV c.m.) drive beam has to be mentioned [4]. This injector option is discussed for the production of a long bunch train (92 μs) consisting of more than 40,000 bunches with a bunch charge of 17.5 nC in a bunch length of less than 20 ps. The needed charge stability is 0.1% rms which requires detailed investigations as described in [5]. These issues will be addressed during the CTF3 program. Although the envisaged laser chain consists of proven technology, a number of technical challenges exist. According to [4], single cathodes have shown that the high current density (21 mA/cm^2), which is crucial for a CLIC drive-beam photoinjector, is achievable.

6.2.2.4 Acceleration to Damping Ring Energy

The pre-bunching and bunching sections of the polarized electron sources are based on existing technology. In case of TESLA the severe thermal loads of the following normal conducting pre-accelerator cavities caused by the almost 1 ms long rf pulses are taken into account. As a result of three dimensional thermal stress analysis, a moderate accelerating gradient below 15 MV/m was chosen. TESLA uses normal conducting cavities up to an energy of 280 MeV in order to allow for solenoidal focusing. The acceleration up to damping ring energy is based on either the TESLA machine or on well known warm S-Band (JLC-X/NLC) or L-Band technology (CLIC).

6.2.3 Positron Source

Two different schemes for the production of positrons are discussed. The CLIC and the JLC/NLC designs are based on a conventional target system similar to the existing SLC positron source [6]. The TESLA design uses a scheme, originally proposed at Novosibirsk [7], where photons are generated by the high energy electron beam in an undulator placed just after the exit from the main linac. These photons are converted into e^+e^- pairs in a relatively thin target.

6.2.3.1 Conventional Layout

The conventional target system of the JLC-X/NLC design uses an unpolarized electron gun. In order to get a sufficiently constant bunch population, a photocathode-based design is chosen which allows bunch-to-bunch intensity adjustments from the source laser. A bunching system is followed by a 10 GeV or 6 GeV drive linac operating at S-Band

frequency, in the JLC-X and NLC, respectively. With the help of an rf separator, the electrons are directed to three out of four quasi-independent target/capture sections. The energy deposited in each target has to stay below the threshold for material damage. This design addresses the risk of target mechanical failure, but it requires that large-emittance, low-energy positron bunches be steered onto a common trajectory with an rf deflector. It may be difficult to achieve the desired throughput and stability of the system because of possible aperture limits of the combiner itself, or other components associated with the combiner.

For JLC-X/NLC, the positrons produced in the shower from each target are collected using a 5.8 T magnetic flux concentrator, overlaid with a 1.2 T dc solenoid field, captured and accelerated to 250 MeV in a 1.4 GHz L-Band linac, combined into the desired bunch train format, and finally accelerated in a 1.75 GeV L-Band booster linac.

For CLIC, the positrons produced in the shower are collected using a 7 T magnetic flux concentrator, overlaid with a 0.5 T dc solenoid field, captured and accelerated to 200 MeV in a 1.5 GHz L-Band linac, and finally accelerated in a 2.2 GeV L-Band injector linac. The technology is described in [8] based on old parameters.

The large L-Band aperture is needed because of the large positron emittance; longer rf wavelength increases the positron capture efficiency.

6.2.3.1.1 Luminosity Issues Because the acceptance of this positron system is large compared to the SLC's, it is possible to achieve the required "yield" (ratio of main linac positrons to electrons) with a reduced drive beam energy (6 GeV (NLC), 2 GeV (CLIC) compared to the SLC's 30 GeV). Simulation studies of the positron production system indicate that the desired yield will be achieved; the simulation codes have been benchmarked against the SLC positron system (NLC), and this allows some confidence in their predictions.

Yield calculations have been performed with complete target-to-damping-ring tracking calculations. Yield is defined as the number of positrons within the pre-damping ring acceptance per incoming electron and GeV. The damping ring transverse acceptance is 0.03 m·rad (NLC) and 0.09 m·rad (CLIC), with an energy acceptance of 1.0% and 2% respectively. The calculated yield is 0.16/GeV and 0.31/GeV respectively.

The positron distribution at the entrance of the NLC pre-damping ring is assumed to be flat. The edge emittance (defined as the maximum transverse action) is 0.03 m·rad (note that the damping ring is designed for a 1.5 times bigger injected emittance to allow for errors).

6.2.3.1.2 Target Fracture Limit Since the total number of positrons required for the JLC/NLC bunch train is almost two orders of magnitude greater than the number of positrons in the single SLC bunch, the previously mentioned multiplexing of target/capture sections is mandatory. A simulation of pulse heating and thermal shock wave in W-Re targets shows that, with fresh nominal tensile strength material, the fracture limit is 70 J/g. The SLC target is about 60 mm in diameter and was operated for 15,000 hours at 120 Hz and 50 J/g before failure. Mechanical tests of the failed SLC target showed that the material was badly fatigued and radiation damaged. The NLC target is designed to receive

less than 50 J/g, and the operational plan avoids operation of the target to the fatigue limit. The number of operating hours required to reach the fatigue limit depends on the target size. The design CLIC [9] energy deposition (42 J/g) is also within the damage limit, provided the target is large enough and replaced often enough.

6.2.3.2 Undulator Source

The TESLA positron injection system [10] has to provide a total charge of 5×10^{13} e^+ per beam macro pulse. Thus it appears that a conventional source is not realistically feasible. The chosen undulator-based positron source uses the high energy electron beam at the end of the main linac. The TDR specifies an undulator length of approximately 100 m where high energy photons are produced with a beam power of typically 135 kW (The NLC group calculates that the specified undulator must be 135 meters in length to produce the desired photon beam [11]. The photons from the undulator hit a thin (0.4 radiation lengths) rotating Ti-alloy target. An adiabatically varying solenoid field is used to capture the produced positrons with a design efficiency of 16% for an initial field of 6 T. Studies of radiation damage and associated lifetime limitations have not been performed.

6.2.3.2.1 Undulator The use of a permanent magnet planar undulator based on existing technology would allow the production of an unpolarized positron beam. The approximately 100 m (135 m) long undulator can be treated as almost conventional since the FEL undulators in preparation for TTF2 as well as for other FELs have tighter tolerances and similar lengths. At DESY and Argonne in a first step, 30 m of undulator will be built. The operation of a 15 m long planar undulator at the TTF-FEL is well understood. Argonne is operating 22 m of undulator, SPring-8 25 m. The LCLS undulator is designed [12] with 100 m length. All these hybrid undulators are more ambitious than the TESLA unpolarized positron source undulator. Technically more ambitious is the possibility to use a superconducting helical undulator that could make polarized positrons available. The TESLA design describes this as an option for a potential upgrade at a later stage of operation. A proof of principle experiment for the production of polarized positrons using a helical undulator is proposed by SLAC [13].

6.2.3.2.2 Positron Pre-Accelerator TESLA proposes to use a normal-conducting standing-wave linac as positron pre-accelerator (PPA). The choice of standing-wave structures is based on a detailed optimization procedure, which has been described together with the final cavity design [14]. Since the cavities have to be operated with 950 μs long rf pulses, the chosen accelerating gradient is moderate (max. 14.5 MV/m). An alternative traveling-wave design is described in [15]. After approximately 55 m the positron beam energy is slightly below 300 MeV, the total capture efficiency from the target to the PPA exit was simulated to be just above 20%. This corresponds to two positrons per 250 GeV electron. This overall yield is reduced at lower electron energies. Therefore the planar undulator cannot be used below about 150 GeV, because it would have to become significantly longer than 100 m.

According to simulations, the positron distribution at the entrance of the damping ring is not flat but more Gaussian-like. The rms emittance is 0.01 m·rad, the edge emittance (defined as the maximum transverse action) is 0.014 m·rad.

Passage through the undulator, placed between the end of the 250 GeV linac and the beam delivery system, causes the energy spread in the electron beam to increase from 0.5×10^{-3} to 1.5×10^{-3} with an average energy loss of 1.2%. The emittance growth is 0.1% in both planes.

It should be noted that, independently of the ILC-TRC, the NLC group has been studying an undulator-based positron source for use in the NLC but have found significantly different positron yields than those described here or in the TDR. These calculations suggest that a 250 GeV e^- beam with a 135-m undulator, would have a yield of 1.8 e^+ per incoming electron if the capture efficiency could be pushed to 25% and the yield with a 160 GeV e^- beam would be 0.6, roughly half of the yield of 1 quoted previously [16, 17]. A capture system efficiency of 25% is also felt to be quite aggressive and an efficiency of 16%, as quoted in the TDR, is more reasonable however the yields will decrease accordingly. Another issue identified by the NLC group is that the potential for radiation damage in Titanium may be significantly higher than in Tungsten and this requires further study. The ILC-TRC was not able to evaluate these differences.

6.2.3.3 Critical Assessments of the Positron Production

The challenge of the positron production in conventional systems is clearly the peak energy deposition in the target. For the undulator-based design the target does not seem to be a critical issue. In addition such a system eliminates the need for multiple targets, may ease the requirements on the pre-damping ring (JLC/NLC design), and provides a straightforward upgrade path to polarized positrons (although challenging in its technical realization). Of principal concern are the logistical issues associated with providing a high-energy electron beam. Also, the linkage between the electron linac, the positron production, the positron damping ring, and the injection into the positron linac has consequences for the machine timing. The corresponding problems were studied [18]. For full performance, the primary electron energy must be above 150 GeV. If lower energy running at maximum luminosity becomes important, then additional electron beam pulses and by-pass beamlines can be used to drive the positron source independently from the lower-energy beam used for the HEP experiment.

The injector commissioning strategy of TESLA includes a low-intensity auxiliary e^+ source for commissioning and machine study purposes. This auxiliary source should be capable of generating a full bunch train of a few percent of the design bunch intensity. In addition, the electron driver of the auxiliary positron source will be built so that full beam loading of the TESLA positron linac can be reached with electrons. Without these measures the initial positron production must await significant progress in the operation of the electron injector and main linac.

The TESLA undulator-based source seems to be well understood from the theoretical point of view, but there remain questions about the specific yields and radiation damage issues. Unfortunately, because of the needed electron beam energy, experiments are not easy to carry out. With respect to a helical undulator for the production of a polarized positron beam, studies could and should be conducted. All projects would benefit from a well-developed technology in this field.

The installation and commissioning of the conventional positron source are independent of the schedule of the electron systems. Nevertheless, for JLC/NLC/CLIC, some part of the commissioning will be done with electrons.

6.2.4 Damping Ring Technology

Although the damping rings rely on common accelerator technology, they all include a number of challenges. For example, the best synchrotron light source instrumentation available is required and there are extreme beam power issues. The TESLA damping ring energy per bunch train is 45 kJ, while for example in PEP II it is 60 kJ. With 5 Hz repetition rate the TESLA damping ring beam power is 0.225 MW. TESLA uses two long damping rings, storing the bunch trains in a compressed mode, with the bunch spacing reduced by about a factor of 16; even with this compression, a large ring circumference of about 18 km is still required. The layout has two 8 km straight sections placed entirely in the main linac tunnel; additional tunnels are used for the 1 km circumference loops at either end. About 400 m of wiggler sections are needed to achieve sufficient damping. Fast kickers with <20 ns rise and fall time are required for compression and decompression of the bunch train at injection and extraction. JLC-X/NLC and CLIC use main damping rings with approximately 350 m circumference. For the positrons a pre-damping ring with large acceptance and about 200 m circumference is added.

6.2.4.1 Key Components

The key components of the damping rings are dipole, quadrupole and wiggler magnets, rf systems, kicker magnets, and beam diagnostic components. From the technical point of view, other critical issues are the impedance of the vacuum system, the alignment tolerances, and overall stability, *i.e.*, magnet power supply jitter, thermal instabilities, *etc.* The discussion of the damping ring-related luminosity issues can be found in Chapter 7.

JLC-X/NLC and TESLA [19] describe beam transport magnets and give specifications for magnet power supplies. All magnets seem to be feasible. The experience from existing damping rings and storage rings seems to be sufficient.

All proposed wiggler magnets are based on permanent magnet hybrid technology. This technology is in use at many synchrotron light sources around the world. The total wiggler length varies from 46 m (NLC) to 400 m (TESLA). Permanent magnets are vulnerable to radiation damage and have to be protected with an appropriate collimation system.

The rf system design of all proposals is based on existing state-of-the-art superconducting (CESR, KEKB) or normal conducting (PEP-II) installations at the B-factories.

Without beam-based correction algorithms the damping ring alignment tolerances cannot be met. The assumed procedure for all LC designs is to align the components with an achievable position tolerance of typically 0.1 mm and a roll angle of typically 0.2 mrad. Then beam-based correction algorithms have to be applied. This subject is discussed in Chapter 7.

6.2.4.2 Kicker Magnets

Because of their beam pulse structure, JLC-X/NLC and TESLA require very different kicker technologies. For TESLA, the kicker rise and fall times determine the size of the damping ring. Pulse-to-pulse stability requirements are similar (few $\times 10^{-4}$) but may be slightly more challenging to fulfill for TESLA.

The demonstrated performance of the SLC kickers was used as a guideline for JLC-X/NLC kicker system specifications. The SLC e^- kickers had 60 ns rise time with two points of equal kick along the flat top separated by about 60 ns. The kickers had substantial (few percent) pre and post kicks (more than one rise time away from the main pulse). The slow rise and fall was caused by the thyratron rise time, circuit elements in the pulser and the impedance of the magnet. The SLC kickers contributed a significant impedance to the rings. Kicker R&D at SLAC has addressed the latter, and pulser R&D for the NLC modulator has addressed the switch and circuit element problems. A magnet has been built. Its impedance has been measured and it will be installed in SPEAR.

SLC kicker amplitude stability was 0.01%, adequate for NLC but still a source of pulse-to-pulse jitter. In order to reduce the jitter for JLC-X/NLC a kicker compensation "achromatic" pair has been included in the design. The system is under test at KEK/ATF and is expected to reduce the effect of the kicker jitter by a factor of 10.

The TESLA damping ring extraction kicker is a critical element. Since the bunches are extracted one by one from the TESLA damping ring, the kicker must have very fast rise and fall times of 20 ns. At present a study with industry aims for an 8 kV, <20 ns flat top, 3 MHz repetition rate pulser to be suited for one 30–40 cm long, 50 ohm kicker magnet. In parallel, a pulser at 1 MHz, <20 ns rise/fall time has been commissioned. Bursts of 2000 pulses, 1 μs distance, 2 kV, 5 Hz burst repetition rate, were produced. At higher voltages, this switch needs better cooling. Therefore the industrial switch is going to be built with an improved cooling system.

Two prototype TESLA kicker magnets were built, a ferrite as well as a stripline kicker, both to be used for testing in combination with the previously mentioned pulser. The vacuum tube is a ceramic tube, the kicker elements are outside the vacuum. After a series of studies and measurements a 600 nm coating was chosen to control the impedance. The kicker field was weakened by less than 3%. The kickers are almost matched to 50 ohms, but for the stripline one might go to 25 ohms in order to increase current and strength. The ferrite-type gives higher fields but cannot be used for pulses shorter than 20 ns. Pulse-to-pulse stability and kicker tails are critical issues and therefore part of the ongoing development program.

6.2.4.3 Vacuum System

The design of the vacuum system has to take into consideration impedance as well as other instability thresholds. In all cases a low impedance design of the vacuum chamber is required. The threshold for microwave instabilities is in both cases, JLC-X/NLC and TESLA, a factor of 2 above the design bunch intensity. The designed impedance Z/n is 30 mΩ or slightly below. Although simulation tools have become much better over the last years, the exact prediction of the impedance is difficult. Therefore all future changes in the damping ring designs should be accompanied by a careful impedance calculation. The detailed technical layout also has to take into account the excellent vacuum pressure of typically 10^{-10} mbar required to limit possible ion effects. Solutions have been worked out for B-factories and synchrotron light sources.

6.2.5 Diagnostics

In a linear collider, beam instrumentation has a greater role than in any other kind of accelerator. Since few tolerances can be met directly in the fabrication and installation process and maintained without using signals from the beam itself, beam instrumentation has the added function of providing the trim information for all subsystems: rf, focusing, positioning and feedback. The beam instrumentation must therefore be reliable and redundant. Furthermore, since both tolerances and beam dimensions are beyond the state of the art for large installed systems, R&D is urgently needed. Instrumentation has been an important part of the linear collider test facility programs, notably at FFTB, ATF and TTF. This work must continue with high priority.

The purpose of beam instrumentation in the linear collider is to validate the performance of each subsystem and to provide input to feedback and optimization controllers. Challenging instrumentation systems are needed for beam position and bunch volume, including phase space orientation. In addition to this, a new type of phase space monitor is required for the measurement of correlations between longitudinal and transverse phase space.

6.2.5.1 Beam Position Monitors (BPMs)

Both BPM resolution and calibration, or control of offsets, are very important for all projects. It is relatively easy to assess single pass resolution, and typical requirements, such as that for NLC (0.3 μm in the linac), are not far from that demonstrated in large systems, such as synchrotron radiation sources. The single pass resolution for APS, scaled to the NLC vacuum chamber size, is 1 μm. Smaller scale tests, like that done at FFTB with cavity BPMs, are considerably better (0.02 μm).

Long term control of offsets, which depends on the system design, has fallen short of the requirements for the JLC-X/NLC linacs and all planned damping rings. System design includes electronic calibration and beam based alignment. It is not possible, at this time, to properly compare performance goals ($\sim$1μm/24 hours) with existing large-scale experience. Small scale tests have been done, also in FFTB, that indicate the goal will be achievable.

For multibunch trains with close spacing (JLC-X/NLC), the required single pass resolution (1 μm) has yet to be demonstrated. For full 714 MHz, bunch-to-bunch separation, resolution of about 5 μm has been demonstrated at ATF. The high-speed multibunch systems will involve state of the art electronic components, will need R&D and are likely to be expensive.

Additional challenges are present with the beam position monitors installed in the cold TESLA accelerator modules. Different types of pickups and cavities have been discussed or tested in TTF. In TTF2 greater focus on the performance of the cavity BPMs will be possible.

6.2.5.2 Profile Monitors

Beam profile monitors provide data on the beam optical match, coupling and emittance for low emittance transport systems. In order to pinpoint error sources the monitors must be distributed along the bunch compressor, linac and beam delivery systems. Profile monitors

in the beam delivery system have special applications, such as at the interaction point, at related upstream focal points and for secondary beams such as bremsstrahlung. Critical performance characteristics that must be tested include:

- Resolution, especially for very high aspect-ratio beams
- Calibration stability (control of systematic errors)
- Durability in very high power density beams
- Operability (the degree to which the measurement interrupts operation)

There is no experience in large systems using profile monitors to accurately uncouple very flat beams, the closest being the wire scanners in the KEK ATF extraction line where the ratio $\varepsilon_y/\varepsilon_x$ is about 1%.

Profile monitor performance comparisons can be readily made for resolution and durability, as shown in Table 6.3.

TABLE 6.3
Comparisons of profile monitor characteristics.

	Resolution	Beam Density Limit	
Wire scanners (Tungsten)	4 μm	3×10^7 @ 1×1 μm	$\sigma_x \times \sigma_y$
Wire scanners (Carbon)	2 μm	3×10^9 @ 1×1 μm	$\sigma_x \times \sigma_y$
Laser wire	0.3 μm	—	
Laser-based interferometer	0.05 μm	—	
Optical transition radiation	2 μm	$5\times10^8/\mu\text{m}^2$	

The typical beam density for NLC is 7.5×10^9 @ 10×1 μm for one bunch and 150×10^9 @ 10×1 μm for the full bunch train. The table does not include beam delivery foci regions. R&D is needed for monitors in these regions.

The laser wire, apparently best suited for linacs, cannot be used to measure vertical sizes of beams having very large aspect ratios because of to the finite waist size or Rayleigh range. The beam at the end of the CLIC linac cannot be monitored using a laser wire for this reason; however locations in the beam delivery system are suitable for laser wire measurements.

Bunch length monitoring has the added challenge that the bunch compressors produce non-Gaussian beam shapes and the detailed shape is important. In addition the bunch length monitors are difficult to calibrate. To meet the challenge of bunch length monitoring, the TTF group has tested a number of techniques based on coherent radiation spectrum and electro-optical sampling. The best calibrated bunch length monitor, based on transverse deflecting structures, has been tested at SLAC and is suitable for all projects. The expected bunch length resolution is 10 μm for low emittance beams. The device is expensive since it requires an rf structure, typically 3 m long, with a high power source. R&D will be done at TTF2 to determine the long term, routine performance of this bunch length monitor.

6.2.5.3 Correlation Monitors

The most common emittance growth mechanism involves an increase in projected phase space through the introduction of a correlation, for example $y - z$. The bunch length monitor described previously can be used to monitor the $y - z$ (or $x - z$) correlation in addition to $E - z$ depending on the nearby optics. The device is an excellent tool for measuring correlations within the beam but it is large and cumbersome to integrate into the lattice and therefore cannot be included in all appropriate places. Another tool for measuring beam correlations is required.

6.2.6 Components of the Beam Delivery System

The Beam Delivery System (BDS) transports the beams from the exit of the linacs to the interaction point, where they are brought into collision, and then safely extracted and dumped in high-power beam dumps. This system must produce the necessary demagnification of the beams, must maintain the beams in collision, and must cleanly extract the strongly disrupted beams after the interaction point, and transport them to high-power dumps. In addition to this the BDS must provide a high level of machine and detector protection, in the event of a linac fault resulting in a beam with either a larger energy error or a large orbit deviation. It also must provide beam halo collimation and sufficient beam diagnostics.

This subsection covers the luminosity diagnostics, but not the overall machine physics aspects of the BDS. Magnets, dump design and collimators are not investigated although some of these components are challenging. The problems are common to all designs and therefore should be handled through close collaborations. Fundamental obstacles are not expected.

Luminosity Diagnostics

The purpose of beam diagnostics in the interaction region area is to monitor the luminosity and provide data on the sources of luminosity limitation. In each design, the luminosity is generated by beam intensity, beam size and by the disruption enhancement. There are a number of phase space dilutions and correlations, as well as stability problems that will cause the pulse-to-pulse and bunch-to-bunch luminosity to fluctuate. It may be possible to experience a drop in luminosity without a direct indication from the upstream beam monitors, if, for example, correlated misalignments are present. The luminosity monitoring system must provide information to help unfold the aberration and pinpoint the cause of the drop.

Luminosity monitors must use the neutral beam emitted from the luminous region (beamstrahlung), the radiative Bhabha signal and secondary processes, such as 2 photon and neutron emission, to perform the task. The first two of these were very useful at SLC, but JLC-X/NLC and TESLA have much more intense beamstrahlung and therefore require a new technology. Furthermore, the details of the beamstrahlung distribution will be used to determine the aspect ratio of the luminous region and the related disruption. For both designs, the beamstrahlung average power is about 300 kW. R&D is needed to make a durable, properly integrated beamstrahlung monitor.

6.2.7 Conclusions

The working group has examined the feasibility of these schemes and subsystems, taking into account the results of the ongoing R&D. This section lists concerns and suggestions for useful R&D.

Concerns and R&D:

- The required laser stability for **JLC-X/NLC**, **CLIC** and the **CLIC** drive beam needs more R&D; the design specifications vary from 2% rms to 0.1% rms. (Ranking 3)
- The target fracture limit for **conventional positron sources** except perhaps for CLIC, which is not far from JLC-X/NLC, must be studied further. (Ranking 3)
- The kickers for the **TESLA** damping rings require ultra-fast high voltage switches. (Ranking 2)
- The **TESLA** beam power at damping ring injection/extraction is high. Injection/extraction has to be stopped immediately in case of a fault. (Ranking 2)
- For all machines, beam position monitor resolution requirements are about 3 times beyond the state of the art, and the (more critical) systematic errors are largely unstudied. Both require R&D. (Ranking 2)
- For all machines, the beam size and luminosity monitors are beyond the state of the art and require R&D. (Ranking 2)
- For the photo-cathode sources, laser improvement for **TESLA** and development for **JLC/NLC** and **CLIC** are strongly recommended. (Ranking 3)
- Studies of the **cathode charge limit** using the E158 beam at SLAC should be continued for **JLC/NLC** and **CLIC**. (Ranking 3)
- The SLAC study of an undulator-based polarized positron source is important and should be carried out, possibly through collaborations. For both JLC/NLC and TESLA the proof of principle, yield, and target issues should be **evaluated**. (Ranking 4)
- The present kicker program for **TESLA** should be strengthened. (Ranking 2)
- For all machines:
  - Existing test facilities should be used to commission new beam diagnostic elements.
  - Challenging issues common to all designs should be addressed through close collaborations.
  - Tracking simulations describing the polarized sources should be checked carefully. There is a history of poor performance at existing injectors. (Ranking 3)
  - Studies of polarized rf photocathode guns should be encouraged. (Ranking 4)
  - A detailed layout up to DR energy should give intensity overhead, location of beam loss, positron beam stability (especially TESLA) and longitudinal emittance. (Ranking 3)

6.3 RF POWER SOURCES

6.3.1 Klystrons

The high power klystrons are among the most challenging components in the rf system for linear colliders, and their development is indeed critical for all the projects at hand. The klystron design parameters, achievements to date, levels of industrialization, and future R&D plans for all five projects are summarized in Table 6.4. The choices of operating frequency and rf pulse performance requirements are naturally linked to those of the corresponding accelerator structures. As a result, there is a clear distinction between the various linear collider projects in their approach to an efficient power source system. All projects, based on normal conducting accelerator technology, adopted pulsed-power systems similar to the original conventional S-band linac technology. They require high-peak power klystrons in the range of 50 to 80 MW with microsecond-long pulses at 100–200 Hz repetition rates. High voltage modulators and klystrons are lumped into single rf units and they are installed together in utility tunnels separate from the main linac tunnel. The klystrons are operated at saturation to improve stability and efficiency. The TESLA rf power source system has to deal with a much longer pulse (millisecond long), since its superconducting cavities are designed to have a half-millisecond filling time. A lower peak power (10 MW) klystron powers 36 cavities with a 1.5 millisecond long pulse at a 5 Hz repetition rate. The low voltage (12 kV) modulators are lumped together in the surface halls spaced 5 km apart along the linac and are connected to their pulse transformers installed close to the klystrons in the tunnel by 12 kV-pulse cables. This configuration eliminates a separate tunnel for the power sources, but in turn requires linac operation to be interrupted for replacement of klystrons. The klystrons are operated at 90% of saturation to provide reserve power for rf feedback.

Among the klystron parameters, the rf efficiency is one of the most important because it determines the quality of a tube. In general, high efficiency is more challenging to klystrons operating at higher frequency, since beams with higher density in a tube behave more nonlinearly because of increased space charge. This makes the design of the klystron (particularly that of the output cavity) much more difficult. Nevertheless, X-band klystrons both at JLC-X and NLC achieved 55% level efficiencies as seen in Table 6.4. The key to this success is the development of the PPM (Periodic Permanent Magnet) focusing system and the incorporation of this technology into the klystron design. Success also comes in large part from the development of new simulation and modelling tools [20]. The PPM focused klystron eliminates the need for power-consuming solenoid magnets, and thus increases the net rf efficiency. Its relatively weak focusing strength demands a lower perveance ($I_0/V^{3/2}$), which in turn makes efficiency even higher. The drawback with a PPM klystron is that it requires a high cathode voltage (480 kV at X-band), raising the burden for the modulators. An alternate approach taken by TESLA is the multibeam klystron (MBK), where seven, low voltage, low microperveance beams are used in parallel in one vacuum vessel [21]. The TH1801 multibeam klystron has achieved an output power of 10 MW at 1.5 ms pulse length with 65% efficiency. It still uses a focusing solenoid, but the solenoid power is only several kW, resulting in only a few percent rf efficiency reduction. The benefit of low perveance can be seen clearly in Table 6.4 where all successful klystrons with efficiencies of 55% or more have a microperveance of 0.5–0.8 mA/kV$^{3/2}$.

TABLE 6.4: Klystron Summary

	TESLA	JLC-C	JLC-X	NLC	CLIC
Klystron type	MBK (7 beams) (Multibeam Klystron)	SBK (Single-Beam Klystron)	SBK MBK in design	SBK Sheet-BK in design	937 MHz MBK for Drive Beams
Focusing system	Solenoid	Solenoid/PPM (Periodic Permanent Magnet)	PPM	PPM	Solenoid
Number of klystrons for two linacs	572	4,276	4,064	4,064	448
Operating frequency [MHz]	1,300	5,712	11,424	11,424	937
Output power [MW]	10	50	75	75	50
Cathode voltage [kV]	110–120	350	480–500	480–500	189
Average rf power [kW]	150 @10 Hz	12.5 @100 Hz	18 @150 Hz	14.4 @120 Hz	100 @200 Hz
Efficiency goal [%]	65	50	55	55	65
Microperveance	0.5 each	1.5	0.8	0.75	0.5 each (6 beams)
Pulse length [μs]	1,500	2.5	1.6	1.6	16.7
Bandwidth [MHz]	n/a	100	100	100	4 (-1dB)
Lifetime goal [h]	60,000 (40,000 h in TDR)	50,000	50,000	>20,000	>25,000
Best performance so far	10 MW, 1.5 ms, 10 Hz @TH1801	53 MW, 2.5 μs, 50 Hz @E3746 No.3	74 MW, 1.4 μs, 25 Hz @PPM-2 65 MW, 1.5 μs, , 53% 50 Hz @PPM-3	72 MW, 3.13 μs, 1 Hz @75XP1 50 MW, 2.4 μs, 120 Hz, 57% @50XP	Design studies
Efficiency achieved so far	65% @TH1801(MBK)	47% @E3746 No.3	56% @PPM-2	56% @75XP1 45% @TH2104(SBK)	Design studies
Lifetime achieved so far [h]	30,000 @TH2104C A year @TH1801 Prototype 2 (4 MW)	2,500 @E3746 No.3	n/a	30,000 @60 Hz@XL-4	Design studies
Power margins	10% for control 6% for waveguide loss	Operated at saturation	Operated at saturation	Operated at saturation	Not studied yet
Vendor's name, if any	Thales, CPI in future	Toshiba	Toshiba	CPI, Toshiba, Marconi	Thales
Level of present industry involvement	High	High	High	Medium (DFM, CPI for 75XP3-2 body)	Design stage
Plan of more industry involvement	CPI VKL 8301 (MBK), UK, Russian, and more	Continue to work with Toshiba	Continue to work with Toshiba	DFM with CPI and other companies	Design stage
Future plan of R&D	Development of horizontal MBK with Thales Study of components to improve lifetime	PPM No.2 More E3746 (solenoid) for SASE FEL (SCSS) Deign of mass production version	PPM-3 in testing Design of PPM-4 (mass production version) More PPMs for J-LUFT project	XP3 in remodelling XP4 in design	Build prototypes

The JLC-C project relies on the more conventional solenoid-focussed klystron, at least in its initial phase.

CLIC is also considering using a multibeam klystron in the drive-beam accelerator [22]. In the present stage of the CLIC project, no prototype klystron and no modulator has been built for their requirements (937 MHz operating frequency, 50 MW output power, 100 μs pulse length, 100 Hz repetition rate, and 65% efficiency, for operation at 3 TeV c.m. energy). Hardware studies will probably begin after the feasibility of the CLIC drive beam scheme has been demonstrated with CTF3. However, Thales has already performed a design study of an MBK tube for this set of parameters. The main result of this study is that a 6 beam MBK with somewhat reduced performance (efficiency of 65% and output power of 40 MW) operating at 215 kV is believed to be feasible.

Although the X-band PPM klystrons produced at JLC-X and NLC have shown more or less satisfactory results in terms of their design output power and pulse length, testing has been generally limited to 25 Hz (PPM-2 of JLC-X) or 1 Hz (XP1 of NLC) repetition rates because of the insufficient cooling systems employed in these prototype designs. However, the latest model for JLC-X, PPM-3, which has a cooling system designed for 100 Hz operation has shown rather promising results in this respect: it so far reached 65 MW at 1.5 μs and 50 Hz with 53% efficiency (PPM-3 is still being tested and performance is not yet limited by the tube characteristics). Its operation is limited to 50 Hz because of the performance of the modulator; the cooling capacity measurements indicate that one can operate it at 100 Hz or even higher repetition rates. The latest version of the 75 MW NLC klystron, the XP3, was designed for 120 Hz, 3.2 μs pulse length operation. However, the two tubes of this design that have been built have had a variety of problems (low gain, oscillations and gun arcing), and are being autopsied to try to understand the causes of their failures. A rebuilt XP3 tube is expected by April 2003, and a more robust design (XP4) should be ready in the summer of 2003. JLC-X and NLC personnel are also designing multibeam or sheet-beam PPM klystrons in order to improve efficiency and lifetime and/or to double the peak power at a much lower voltage.

Both high power PPM klystrons and multibeam klystrons are very new technologies in the industrial world, and the increased complexity of these tubes may cause higher construction costs as well as higher failure rates. Lifetime testing has only recently started for all linear collider projects. Among these tests, the JLC-C E3764 No. 3 klystron achieved more than 2,500 hours of accumulated operation without a major failure [23]. The 50 MW X-band solenoid-focusing XL4 klystrons have been operated cumulatively over 30,000 hours at 60 Hz at the NLCTA. The first TESLA MBK TH1801 has operated for about 5,000 hours with reduced performance (4 MW-output power, 1.5 ms-pulse length, and mostly 1 Hz repetition rate). It was also operated at the full specifications over several weeks. However, these achievements are still far from the desired lifetime goals in the range of several tens of thousands of hours. S-band experience with the SLAC 5045 klystron [24] (65 MW peak power, 27 kW average power, 350 kV beam voltage, and 40,000 hours lifetime) indicates that similar lifetimes may eventually be achievable. The S-band experience at SLAC also shows that the most likely cause of klystron failure is cathode arcing due to barium evaporation and deposition on the anode surface. The cathode lifetime is also related to its operating temperature: every increase of 25°C cuts its lifetime in half. Some industrial companies such as Thales have also investigated the lifetime issue in detail as part of a study of klystron mass-production. According to their study, the cathode emission is the

main factor affecting the lifetime of the TESLA MBKs as opposed to barium (the second TESLA MBK TH1801 failed recently due to gun arcing). They are planning cathode studies aimed at increasing their lifetime beyond 40,000 hours. The problem with verifying lifetime of this length is that several years of operation are required. All available studies should be centralized, compared and analyzed so that more accurate predictions of lifetime can be made from various klystron designs and short-term operational data.

The total number of klystrons required for linear colliders is such that industrial involvement is clearly needed for mass production. However, the specifications of klystrons for linear colliders are much more demanding than those for any klystron now commercially available. Thus the involvement of commercial klystron manufacturers from an early phase of R&D is very important to allow them to become familiar with the idiosyncrasies of high-peak power klystrons. The required level of industrialization of klystron production is high for all LC projects. TESLA, JLC-C and JLC-X have successfully produced klystrons through their various industrial partnerships. At TESLA, industrial involvement is expanding, with several proposals in the works. Both JLC-C and JLC-X have worked intensely with Toshiba and will continue to work with this company to refine their designs and reduce costs. NLC has launched the so-called Design For Manufacturing (DFM) klystron program with industry during the past three years to produce lower-cost 50 MW and 75 MW PPM klystrons. The involvement of multiple manufacturers for each project will help reduce acquisition costs via competitive bids. Soon, CPI will join the companies manufacturing MBKs and PPM klystrons, of which Thales, and Toshiba, respectively, are the dominant producers. The international microwave klystron industry is thus gaining experience that it will need to handle the large klystron orders from any of the linear collider projects.

6.3.2 Modulators

Modulators are also critical components of the rf power system. Like all the rf subsystems, high efficiency, high reliability, and low cost are the goals for successful modulator design. The design parameters, achievements to date, the level of industrialization, and future R&D plans of all 5 projects are summarized in Table 6.5. The design parameters and the stability requirements of the associated DC power supplies are summarized in Table 6.6. Modulators used to be dominant cost drivers in the JLC-X and NLC designs when line-type modulators were initially envisioned. Line-type modulators like those used in the SLAC linac have some major deficiencies. The thyratron switch tube needs frequent tuning and has a short lifetime of around 15,000 hours. The thyratron is a fast ON switch, but is slow to turn OFF. The overall efficiency of this type of modulator is as low as 50–60% because of the large losses in the various components and the relatively slow pulse rise and fall times due to their high ratio step-up transformer. The Pulse-Forming Network (PFN) needs a large number of parallel LC circuits to get good pulse flatness. For a 1.5 ms long pulse for TESLA, the size and cost are quite high.

An approach that mitigates many of these problems, which was adopted at NLC and later at JLC-X, is to use the fast ON-OFF Insulated Gate Bipolar Transistor (IGBT) as the power switch and to incorporate that technology into an induction-linac type modulator design. The IGBT switch is anticipated to have a longer lifetime than the thyratron. The solid-state induction modulator is basically a large stack of small pulse transformers in

TABLE 6.5: Modulator Summary

	TESLA	JLC-C	JLC-X	NLC	CLIC
Modulator type	Bouncer Solid-state switch (IGBT)	Smart modulator Thyratron switch	Linear induction Solid-state switch (IGBT)	3-turn induction Solid-state switch (IGBT)	Line-type with double PFN and two thyratrons
Transformer ratio	1:12	1:16	1:1	1:3	1:10
Output peak voltage [kV]	130	400	500	500	190
Output peak current [A]	150	317	2120	2120	250
Number of klystrons to be fed	1	1	8	8	1
Pulse flat top [μs]	1,500	2.5	1.6	1.6	16.7
Rise and fall time [μs]	200	1–2	0.2	0.2	<4
Pulse flatness during flat top	$< \pm 0.5\%$	$< \pm 0.5\%$	$< \pm 0.3\%$	$< \pm 1\%$	$< \pm 0.1\%$
Pulse to pulse voltage fluctuation	$< \pm 0.5\%$	<1% (p-p)	$< \pm 0.1\%$	$< \pm 0.1\%$	$< \pm 0.1\%$
Efficiency goal [%]	85	>60	>80	>80	95 w/o charging supply auxiliaries and solenoids
Reliability (MTBF) goal [hours]	100,000	n/a	>10,000	>10,000	n/a
Best performance so far	128 kV, 89 A, 1.7 ms, 10 Hz @TTF3, 117 kV, 131 A, 1.7 ms, 10 Hz @TTF1,2	350 kV, 2.5 μs, 60 Hz @Smart No.1	Design studies	500 kV, 650 A, 2.5 μs, @4-Dog	Design studies
Pulse flatness achieved so far	$< \pm 0.5\%$	$< \pm 0.5\%$	Design studies	n/a	Design studies
Pulse to pulse voltage fluctuation achieved so far	$< \pm 0.5\%$	n/a	Design studies	n/a	Design studies
Efficiency achieved so far	>85% @TTF3	>52.4% @Smart No.1	Design studies	>80% @4-Dog	Design studies
Lifetime achieved so far [hours]	35,000 @10 Hz@TTF3	15,000 @Smart No.1	Design studies	n/a	Design studies
Vendor's name, if any	PPT, ABB, FUG, Beerwald	Nihon Koshuha	Mitsubishi	In house production	Design stage
Level of present industry involvement	High	High	High	Medium. Bechtel for engineering design	Design stage
Plan of more industry involvement	Already ongoing with PPT, ABB, FUG and Russian	Continue to work with Nihon Koshuha	Already ongoing with Mitsubishi and Hitachi	n/a	Design stage
Future plan of R&D	Modular layout. Enhance reliability and maintainability. Intelligent diagnostics and interlock to improve lifetime.	Smart modulator No.2. Modular design. Closed type for SASE FEL. Improve reliability and lifetime of thyratron.	4-Pack by mid 2003. 50 kV prototype by mid 2002. High voltage IGBT with faster rise and fall time. Reliability.	8-Pack modulator for 8-Pack Project Phase II by mid FY2003. Cooling. Reliability. Circuit and klystron protection.	Build prototypes.

TABLE 6.6
Power Supply Summary

	TESLA	JLC-C	JLC-X	NLC	CLIC
Charging voltage [kV]	10	47	3.2	4	45
Average power [kW]	150	39	313	500	151
Efficiency [%]	>94 (HVPS)	n/a	96	96	>92
Stability [%]	0.5 (p-p)	±0.13	±0.1	±0.1	±0.1

which the primaries of the cores are driven in parallel by separate sets (called cells) of IGBT switches and capacitors operated at relatively low voltage (2–4 kV), and the high voltage is developed at the secondary in series [25]. The idea is so simple and flexible that the same design can be used for different voltages and pulse lengths with minimum changes, unlike the line-type modulators where the whole system, in particular the PFN, would need a major change. The driver cell (an IGBT switch and two capacitors on a printed circuit board) is designed as a plug-in module that can be easily accessed and replaced in the field for fast maintenance. Additional driver cells are installed as hot spares to enable longer periods of continuous operation without interruption for maintenance. NLC has already built a 4-pack prototype with a 3-turn secondary and has demonstrated an efficiency of about 80% and a pulse shape with fast rise time of about 300 ns (fall time is slower). JLC-X has adopted a similar design, but uses a single-turn straight secondary with a simpler insulation design and lower cost of the secondary conductor, in exchange for more cores. To compensate a 2% voltage droop during the flat top, an appropriate fraction of IGBT drivers is triggered with programmed delays resulting in a pulse flatness of ±0.3%. This level of pulse flatness during the flattop, as well as $< 0.1\%$ pulse-to-pulse voltage fluctuations, are required to keep the rf-to-beam phase error below 1°.

There are many other technical issues to be addressed and investigated such as IGBT protection and reliability in the pulsed-power operation where the IGBT drivers are not well modelled (very high dI/dt, peak current, high voltage lasting for only a few microseconds, *etc.*). The diode testing is underway at SLAC to look for signs of arc damage under controlled faulting. In the first high voltage test, about 20% of IGBT drivers were damaged by a single arc, seemingly because of ringing in the 3-turn secondary when the klystron faulted. Even after installing snubbers to compensate the mismatch, single IGBT driver failure was found to occur. It stopped only after the EUPEC IGBT drivers, found to have an unbalanced induction layout inside, were replaced with more balanced and higher voltage rated Mitsubishi drivers. Since then, the NLC 4-pack modulator is producing 400 kV-1.5 μs long pulses for the 8-pack Phase-I project with no apparent degradation. The production cost per klystron when driving 8 klystrons with a single induction modulator is estimated to be lower than for a 2-pack line-type modulator by a factor of 2–3. The latest cost estimate shows that the modulators are no longer the largest cost driver at NLC and JLC-X compared to other rf components.

The induction technique described previously cannot be applied to a millisecond long pulse for TESLA, since it would require a large amount of magnetic material and/or a large number of secondary turns to avoid saturation. Instead, a classical twelve-to-one turns ratio

transformer is used although the primary is driven using solid-state switches. To avoid having very large storage capacitors to achieve good pulse flatness ($< \pm 0.5\%$) during their long (1.5 ms) HV pulses, a bouncer circuit is used [26]; otherwise the droop of 19% on the main capacitor bank during the pulse would produce an intolerable pulse distortion. This modulator consists of a DC power supply (10 kV), a main capacitor bank, a bouncer circuit, two solid-state switches, one for the main capacitor bank (IGBT or IGCT, Integrated Gate-Commutated Thyristors) and another for the bouncer circuit (SCR), and a pulse transformer. The bouncer circuit is basically a resonant LC circuit producing a single sine wave to compensate for the main capacitor droop. Several bouncer-type modulators were built and are in use at TTF. They have shown more than 85% efficiency at a pulse length of 1.7 ms with 200 μs rise and fall times at 10 Hz. They have also achieved a pulse flatness of $< \pm 0.5\%$ and a pulse-to-pulse voltage fluctuation of $< \pm 0.5\%$. A klystron-modulator unit has an interlock system in the event of a klystron gun spark. To ensure that the energy deposition in the spark remains below 20 J to avoid damage to the klystron gun, the relevant IGBT switch will be immediately opened to disconnect the capacitor bank from the sparking klystron. The energy stored in the transformer leakage inductance and the power cable will be dissipated in two networks of resistors. Five modulator/transformer/klystron systems are operational. One modulator at TTF has been working since 1994 for about 35,000 hours of operation at a 10 Hz repetition rate, and is still in operation. The use of IGBT switches assures high reliability. The location of modulators in the surface halls allows for fast repair in case of problems. The next phase of development will be the design of a modular layout to allow for fast exchange of components and to further enhance reliability and maintainability.

Because of the long pulse length for TESLA, the size of the pulse transformer core is large, since it is proportional to the product of the voltage and the pulse length. The transformers are placed in the tunnel, close to the klystrons. A design already exists for a transformer, which fits the tunnel layout, but the connectors, which should allow quick exchange in the tunnel, remain to be designed. The maximum distance of pulse delivery from the modulator to the transformer in the tunnel is about 2.8 km. The power loss in the HV cable will be 2% on average. There is a concern of pulse shape distortion, in particular at the leading edge of the pulse, if the cable impedance is not matched to the klystron impedance and the skin effect of cable inner conductor is not minimized [27]. The cable must be designed for the appropriate dV/dt conditions, but the voltage is quite low (12 kV), and the insulation should therefore be no problem. If the design and the fabrication are done correctly, then the HV cable is not regarded as a significant concern. The prototype cable was ordered, and the testing will start soon.

At CLIC, a conventional line-type modulator with a double PFN and two thyratron switches has been studied to drive a single 50 MW multibeam klystron [22]. They are also investigating alternative modulator designs using solid-state switches as a future replacement for the thyratrons.

As is the case of klystrons, the involvement of industry at an early stage to build prototypes of critical components or integrated systems is very important to familiarize manufacturers with the new technologies. A series of Modulator Workshops have been held in the US during which industrial designers and manufacturers have been introduced to the requirements of the linear collider projects. TESLA is already working with several companies (PPT, ABB, FUG, and Beerwald) to deliver subunits of the latest bouncer

modulators. PPT could now take over the task to build and deliver a complete modulator. JLC-C and JLC-X have been producing their modulators in industrial partnerships with various companies (Nihon Koshuha, IHI, Mitsubishi, and Hitachi), beginning with the initial design. NLC has contracts with Bechtel-Nevada to provide a detailed mechanical engineering design and sophisticated machining capabilities. Bechtel has also contributed to the fabrication of several prototype solid-state induction modulators in collaboration with LLNL. The industrialization of the linear collider modulators is well under way, worldwide.

6.3.3 Low-Level RF Control

The requirements for the low-level rf (LLRF) control system are defined in terms of phase and amplitude stability of the accelerating field during the flat top portion of the rf pulse. The stability requirements, the status of the design and hardware developments, and future R&D plans for all five projects are summarized in Table 6.7. All projects rely on beam induced signals to adjust the phase of the rf at the structures. Superconducting rf cavities require more complex low-level control than normal conducting systems. Both feed forward and feedback loops are needed and the LLRF system must be carefully specified in order to avoid unnecessary complexity and retain the needed flexibility.

For both TESLA and JLC-X/NLC there must be a system that distributes a reference clock that is accurate enough to allow the acceleration of a pilot beam bunch through the linac. A successful demonstration of a fiber optic based X-band distribution system was done at SLAC. The system uses two way optical transmission on a fiber with an active feedback system for compensation. Both beam pickups (in the JLC-X/NLC) and signals from the accelerator structures themselves (in all machines) are used to control the fine phase adjustment of the structure.

At TESLA, it is desirable to keep the bunch-to-bunch energy spread below 5×10^{-4} in order to assure that the single-bunch chromatic effects do not become a dominant emittance growth factor. This requires tight control of the accelerator field in the vector sum of 36 cavities (one klystron unit) on the order of 0.03% (correlated errors) and 0.5% (uncorrelated) for the amplitude and 0.2° (correlated) and 3° (uncorrelated) for the phase. The major sources of perturbations at TESLA are fluctuations of the bunch current and changes in resonant frequency resulting from the deformations of the cavity walls which can be induced by mechanical vibrations (microphonics) and Lorentz forces (at TTF, the effect of microphonics is small compared with Lorentz detuning). The amplitude and phase errors due to the Lorentz force (and microphonics) are on the order of a few % and 10°–20°, respectively (without piezoelectric tuners). The non-repetitive errors due to bunch charge variation and microphonics are much smaller than those due to the Lorentz force detuning. The feedback scheme works at the design gradient of 23.8 MV/m, but the additional power required for field control at the planned upgrade to 35 MV/m will exceed the klystron power reserve of 10%. However, the repetitive time-varying Lorentz force detuning can be reduced by more than one order of magnitude by using a piezoelectric tuner in an adaptive feedforward way, as successfully demonstrated by a recent experiment at TTF. This scheme will reduce even the 10% power reserve needed at the nominal operating gradient.

TESLA developed a digital LLRF system using an I/Q modulator scheme to control both the in-phase (I) and quadrature (Q) components of the cavity field [28]. The I/Q concept

TABLE 6.7: Low-level RF Control System Summary

	TESLA	JLC-C	JLC-X	NLC	CLIC
RF-to-bunch phase stability	<0.5degree	n/a	1 degree	1 degree	0.25 degree
Pulse-to-pulse phase stability	<0.5degree	n/a	1 degree	1 degree	0.25 degree
RF amplitude stability [%]	<0.03	n/a	<0.1	<0.1	<±0.1
Power routing changing speed [ns]	3–4,000	n/a	10	10	n/a
Main source of errors	Lorentz-force detuning. Microphonics. Bunch current fluctuation.	n/a	Thermal expansion of rf structures and delay lines. Beam-loading. Modulator voltage ripple.	Thermal expansion rf structures and delay lines. Beam-loading. Modulator voltage ripple.	Have to be found with CTF3.
Design type	Digital I/Q modulator	n/a	To be decided.	Digital IF techniques.	n/a
Status of design	Concept proved by TTF1. To be implemented in TTF2.	n/a	Under way.	Under way.	Prototype under construction for CTF3.
Status of hardware and testing	Studies under way.	n/a	Cavity BPM tested at ATF.	Prototypes planned.	Ready by end 2002.
Future plan of R&D	Work on adaptive feed-forward. System identification. High level automatization. Piezoelectric tuning mechanism. Cost reduction. Improve redundancy.	n/a	System test at ATF linac using a beam. Improve redundancy for cost reduction.	High speed DAC/ADC module. A full 8-pack test planned.	n/a n/a

allows for detection and control in all 4 quadrants including zero, and is most suitable for the control of large cavity detuning since it minimizes the coupling between loops. The rf signals from each cavity are converted to an intermediate frequency (IF) of 250 kHz and sampled at a rate of 1MHz to provide digital I/Q information for individual cavity fields. The vector-sum of 36 cavities is calculated using digital signal processing (DSP) and the amplified error signal is combined with the feedforward signal and fed back to the vector modulator that controls the klystron input-power driver. The digital technique allows for calibration and corrections to be made and updated. In this method, all 36 cavities driven by a single klystron are treated like one cavity and the feedback algorithm is applied only to the vector-sum. Therefore, fast control of an individual cavity field is not possible. The major advantage of the digital feedback is the built-in diagnostics, which is essential for the operation of 36 cavities driven by one klystron. The phase calibration of individual cavities and the vector sum are measured relative to the beam by measuring the beam loading induced in the cavities. This can be done at a total charge of 200 nC presently; the goal is to get as low as 8 nC for calibration.

A smaller-scale LLRF system was implemented at TTF with 16 cavities and it was demonstrated via beam measurements (typically 0.15% rms energy fluctuations during the macro-pulse and 0.25% pulse-to-pulse) that the $<2\times10^{-3}$ amplitude stability and <0.5% phase stability required at TTF can be achieved with a (dead reckoned) feedforward table and the feedback system. The residual errors were dominated by repetitive factors that were reduced by the feedforward by about one order of magnitude. These results show promise that the tight requirements on amplitude and phase stability at TESLA can be achieved by the combination of these feedback and adaptive feedforward systems. An improved digital controller for the TTF LLRF is under development. In the new system, a single digital signal processor replaces the six used in the prototype. It will be used to increase the system flexibility and to more effectively apply modern technology.

At JLC-X and NLC, the rf modulation system is used as a fast phase shifter, since the klystron is operated at saturation and the rf output is thus kept at a constant power level. The rf amplitude stability must be provided by control of the modulator pulse amplitude and is expected to be better than 0.1% pulse-to-pulse. The objective of the JLC-X/NLC LLRF system is therefore to compensate the beam-loading effects, the repetitive phase variations during the pulses due to modulator voltage ripple, and the phase drifts caused by thermal expansion of the accelerator structures and the SLED-II power delay lines. The goal of phase control is to achieve a 1° rf-to-bunch setting accuracy and a 1° pulse-to-pulse stability.

At JLC-C an additional antisymmetric phase modulation is needed to produce an AM modulation at the input of the compressor which compensates for its intrinsic distortion.

Unlike TESLA, JLC-X and NLC use a SLED-II pulse compression scheme to drive four pairs of klystrons to individually deliver rf power to four accelerator structure clusters (each consisting of six structures) in the proper sequence, synchronous with the beam. The compression of rf power is achieved for SLED-II by quickly modifying the relative phase of the klystron drive during each pulse. The wide bandwidth of the system (>100 MHz) allows rapid phase changes in about 10 ns. Even with a state-of-the-art stabilized fiber optics rf reference/distribution system, there will still be phase drifts present in the system. In order to optimally phase the rf pulse going to each rf structure cluster in the presence of phase errors and drifts, the absolute phase of the accelerator rf will be determined by

measuring the relative phase with the respect to the beam. The rf-to-beam phase is monitored using rf detectors on the structure outputs. This signal is fed back to the klystron driver so that the phase of the rf pulse going to each rf structure cluster can be adjusted individually. Thus, six structures in one rf cluster are treated like a single structure with respect to the fast phase feedback. The phase differences among the six structures in the same rf cluster are set initially and not adjusted thereafter.

At NLC, programmable high speed digital IF techniques are planned for both arbitrary klystron drive modulation and accurate rf vector detections, rather than the I/Q approach currently used at NLCTA, in order to reduce system cost and improve accuracy [29]. Prototype studies have just begun and have produced some encouraging initial test results. A full 8-pack test installation is planned. At JLC-X, the beam-based phase stabilization system for rf pulse transmission through the SLED-II lines is under development. A cavity beam pickup has been developed and a test result at the ATF linac demonstrated that it can detect the beam phase within 1°. At CLIC, prototypes of LLRF systems are under construction for CTF3. They should be ready by the end of 2002.

6.3.4 Conclusions

6.3.4.1 TESLA

Both Thales MBK klystrons and bouncer modulators met pulse performance requirements (peak power for klystron or peak voltage for modulator, pulse length, efficiency, repetition rate) for TESLA. However, the lifetime of the MBK klystron has not yet been demonstrated.

R&D (Ranking 3):

- The lifetime test of the MBK klystron, particularly because of cathode degradation, should be pursued as planned.
- The improvement of the LLRF system design should be given high priority.

6.3.4.2 JLC-C

The repetition rates of the klystron and the modulator need to be improved to meet design requirements (100 Hz).

The efficiencies of the klystron and the modulator need to be improved to meet design requirements (50% including solenoid-power and 65%, respectively).

R&D (Ranking 2):

- The operation of the klystron and modulator at 100 Hz repetition rates should be demonstrated.
- The LLRF system needs to be designed and demonstrated.

- The lifetime tests of the klystron and the modulator should be pursued as planned.

R&D (Ranking 4):

- The development of the C-band PPM klystron should be supported and continued.
- Some R&D may also be necessary for a new modulator design with a solid-state switch to improve the pulse shape efficiency and to minimize the time for maintenance.

6.3.4.3 JLC-X/NLC

The latest test result of the JLC-X PPM klystron is gratifying and looks promising.

The latest test result of the NLC 4-pack induction modulator prototype is looks encouraging. More klystron arcing tests are needed to verify the protection circuit of the IGBT switches.

R&D (Ranking 2):

- The operation of the JLC-X PPM klystron at 150 Hz (JLC-X) or 120 Hz (NLC) repetition rates needs to be demonstrated.
- The operation of the NLC induction modulator at full specifications needs to be demonstrated.

R&D (Ranking 3):

- NLC should continue its current PPM klystron R&D to achieve pulse performance and repetition rate requirements. Since the lifetime test is yet to be performed, development of this alternative design to the JLC-X PPM klystron should be continued.
- Development of the JLC-X linear induction modulator should be supported and pursued as planned as an alternative design.
- The improvement of the LLRF system design should be given high priority.
- The lifetime tests of the klystrons and the modulators should be pursued as planned.

6.3.4.4 CLIC

Neither drive beam prototype klystron nor modulator has been built so far and both are still in the paper study stage. Hardware studies will probably not begin before the feasibility of the CLIC drive beam scheme has been demonstrated with CTF3. Thales has a design study of a 6 beam MBK with somewhat reduced performance that needs to be demonstrated (937 MHz-operating frequency, 40 MW-output power, 16.7 μs-pulse length (500 GeV c.m.), 100 Hz-repetition rate, and 65% efficiency). It must be noted, however that

more klystrons can be used if the peak power requirements cannot be met. The 90% design efficiency for the modulator will be difficult to achieve with the conventional line-type modulator that is currently under consideration.

R&D (Ranking 2):

- R&D study of an MBK tube including prototyping should be started for the 3 TeV upgrade.

R&D (Ranking 3):

- A more efficient type of modulator should be studied for the 3 TeV upgrade.

6.4 RF POWER DISTRIBUTION

6.4.1 TESLA

For TESLA-500, the rf power is generated by 10 MW klystrons having two output windows, operating at 1.3 GHz, and providing an rf pulse of 1.37 ms at a repetition rate of 5 Hz. The rf waveguide system distributes the rf power to 36 nine-cell superconducting cavities per klystron. Thus, the basic rf unit consists of one klystron feeding 36 standing-wave cavities. Each cavity transfers 231 kW to the beam during the 0.95 ms long beam pulse. Each linac contains 286 of these units.

The rf distribution is a linear system branching off identical amounts of power for each cavity from a single line by means of directional couplers. Further functions of the waveguide system are to protect the klystron from reflected power, to avoid cross-talk between the cavities and to allow proper phasing and impedance matching. The latter function is provided in each branch by a three-stub waveguide transformer, which has each stub equipped with a motor remotely controlled by the low-level rf system.

Since not all cavities will reach the same accelerating gradient, the worst performing cavity in the group of 36 cavities limits the gradient. In principle, this can be mitigated by:

- Grouping cavities after acceptance tests (all cavities are tested in vertical cryostats)
- Detuning particular cavities
- Developing adjustable hybrid couplers plus tuners

The rf distribution is not under vacuum but in air; the cavity vacuum is isolated from the distribution system by the two rf windows in the main coupler.

A detailed description can be found in Chapter 3. Figure 6.1 gives the schematic layout of the system.

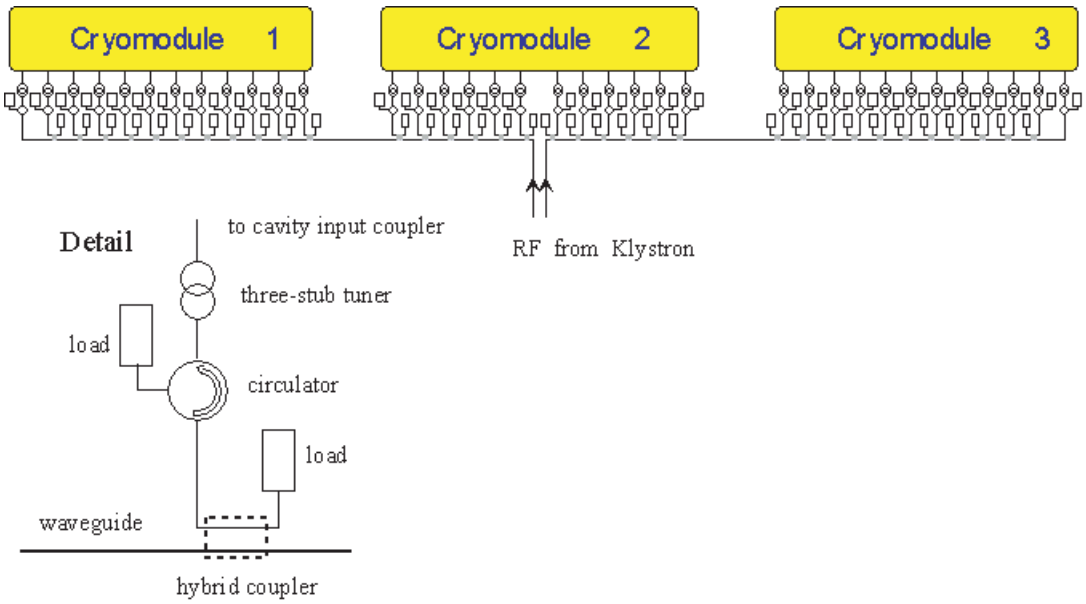

FIGURE 6.1. Schematic layout of the TESLA waveguide distribution system

The advantages of the concept are:

+ Simple, modular, proven technology for hybrid, circulator, tuner and loads
+ Used in TTF, similar to the rf system in the electron ring of HERA (though not pulsed)
+ No need for pulse compression
+ High efficiency (higher than tree-like distribution)
+ The rf power in the components is relatively low
+ No vacuum or overpressure in the distribution system which facilitates change of components
+ Low number of klystrons (572 in total)

Its disadvantage is:

– 36 cavities are off in case of a klystron or modulator fault leading to a drop of 0.87 GeV (0.35%) in beam energy

All the components are already in use in TTF1 at nominal power and comply with the specifications for TESLA 0.5 TeV.

In order to save costs, to improve engineering margins, and to improve performance, alternative and complementary designs for the following components are being developed:

- Three designs for adjustable (±1 dB) hybrid couplers to match the power to different cavity quench thresholds. High-power tests are planned for 2003/2004;
- A magic tee E-H tuner as waveguide type transformer instead of the three-stub plunger for higher power capability independent of the transformation ratio, providing a phase shift range of ±180°. High-power tests are foreseen in November 2002;
- The use of welding techniques instead of flanges for cost reduction and improved reliability. Tests of this technique are foreseen in 2004.

The waveguide system has to operate at a higher peak and average power for TESLA upgraded to 800 GeV, where each branch has to sustain 0.7 MW peak and 8 kW average forward power instead of 0.35 MW and 5 kW respectively. In case the superstructure concept is adopted, these values increase to 1.3 MW peak and 14 kW average.

- Experience exists with waveguides at the required power levels (test at DESY done).
- The hybrid couplers have to be tested at the higher power (tests foreseen in 2004).
- Alternatives exist for the circulator: either the circulator is pressurized with nitrogen or a new circulator is designed. The former has been tested and peak values of 4 MW have been reached albeit with a reduced repetition rate. Further developments of this approach are foreseen. The design of a new circulator is pursued together with three firms. The designs will be completed in 2002 and first tests are foreseen in 2003.
- The loads have been tested up to 10 kW which is sufficient for 800 GeV, but not quite sufficient for use of the superstructure at 800 GeV. However, commercially available loads exist for the latter application.

6.4.2 JLC-C

The power distribution system combines the outputs from a pair of 50 MW klystrons operating at 5.712 GHz in a 3 dB hybrid, increases the peak power to 350 MW by an improved SLED-type rf pulse compressor and splits the power with three magic tees in order to power four TW accelerator sections. Thus, the basic rf unit consists of two klystrons feeding four accelerator sections. Such a unit is also the smallest possible vacuum unit separated by two gate valves from the adjacent accelerator sections.

Each linac consists of 989 of these units. The layout of this rather classical system is shown in Figure 3.22 in Chapter 3.

The most demanding part of the system is the rf pulse compressor which is of a novel design. It consists of a coupled cavity chain acting as a delay line and comprising two storage cavities ($TE_{01,15}$ mode) coupled by a cavity operating with the $TE_{01,05}$ mode in between. The phase advance has been chosen to be $\pi/2$. The coupling irises between the cavities limit the group velocity. However, they cause frequency dispersion in the

propagating wave, which would result in a large distortion of the output waveform if not compensated by AM modulation of the input to the compressor. This amplitude modulation is produced by an anti-symmetric phase modulation of the input to the two klystrons and produces a compressed output pulse with a flat top of about 500 ns.

It has been shown recently that this phase modulation can be used to also take advantage of the rf power produced during the rise time of the modulator. Cold model measurements indicate that this new modulation scheme increases the compression ratio from 3.25 to the desired factor of 3.5. The expected power efficiency is larger than 70%. A further increase of the efficiency is conceivable by using larger storage cavities but no definitive R&D plan exists for this development.

The advantages of the system are:

+ Its simplicity as far as the high-power hardware is concerned
+ Shorter waveguide lengths than other pulse compression systems
+ Since the size of one rf unit is rather small, testing of one full rf unit is relatively easy
+ If one rf unit stops, then the energy drops only by 0.25 GeV (0.1%)

Its disadvantages are:

– The inherent lower rf efficiency of this SLED-type pulse compression
– Large number of klystrons (3956 in total compared to 448 of CLIC or 572 of TESLA)

In order to limit the critical detuning of the cavities forming the pulse compression system due to variations of the operating temperature, cavity models made from copper-plated invar have been developed but they have not yet given fully satisfactory results. New cavities for the high power test are under design.

The standard waveguide components such as bends, couplers and flanges have been developed and will be tested under nominal power in 2003 to 2004.

One rf unit will be tested at full power in 2004 in preparation for the C-band linac foreseen to drive the FEL of the SPring-8 Compact SASE Source (SCSS) by RIKEN. This will demonstrate the feasibility of the rf pulse compressor at high-power; it will also test the stability and reliability of the whole unit under operating conditions, including the robustness of the approach to control phase and amplitude of the klystron outputs.

The planning of SCSS foresees a full test of the first part of the linac consisting of the L-band injector and one C-band unit providing 300 MeV electron beam in 2005. This will be an excellent opportunity to test the C-band system under operational conditions and provide precious information on the possible design improvements to be made for a linear collider.

The original upgrading to higher energies foresaw the development of klystrons with twice the power and an extension of the linac by a factor of $\sqrt{2}$ in order to reach 1 TeV in the center-of-mass. Since this klystron development is not so obvious and the efficiency of an X-band linac is superior, the most probable upgrade path of a 0.5 TeV C-band collider is

the addition of an X-band part. Hence, no specific C-band development for the upgrade is required. Since there will be sufficient time for the development, a Delay Line Distribution System (DLDS) can be envisaged for this upgrade which has a higher efficiency than the compact SLED system.

6.4.3 JLC-X/NLC

6.4.3.1 Baseline Design

The basic rf unit consists of one modulator, four pairs of 75 MW klystrons operating at 11.4 GHz, a SLED-II type dual mode rf pulse compression system, and the waveguide distribution system. Each pair of klystrons delivers an rf pulse of 150 MW and 1.6 μs duration to a SLED-II system, which compresses the pulse by a factor of 4 to the required 0.4 μs using two 29 m long delay lines operating with the TE_{01} and TE_{02} modes. The 450 MW output pulse is fed through a low-loss circular waveguide and four magic tees to a girder containing six accelerator structures. Thus, the basic unit is composed of one modulator and 8 klystrons feeding 24 accelerator sections.

Each linac consists of 254 such rf units. The total length of the beam line pertaining to one rf unit is about 26.0 m of which 21.6 m is active length. The length of the delay lines exceeds the length of the beam line because the present layout is not yet optimized.

Originally, it was proposed by JLC-X and NLC to use the more efficient Delay Line Distribution System (DLDS) as the pulse compression system instead of SLED. It has an expected compression efficiency of about 85%. However, testing of a full system would have required a substantial investment since the basic units are relatively large. Furthermore, it was deemed that the time required to fully develop and test such a system would be unacceptably long. Also the multibranch vacuum system of the DLDS system has an extension which gave rise to concern. In particular, the demonstration of the dual-moded DLDS of NLC would have required eight 75 MW klystrons with a pulse length of 3.2 μs instead of only two 75 MW klystrons with a shorter, and therefore, much easier to obtain pulse length of 1.6 μs, which is sufficient for a demonstration of the preferred dual-moded SLED-II system. In addition, there is already a lot of experience with the SLED-II system though it has always been only single-moded and its dual-mode operation remains to be demonstrated. For these reasons, it has been decided to choose the simpler and probably more robust SLED-II solution.

The advantages of the scheme are:

+ A lot of operational experience exists with SLED-II in NLCTA
+ The power in the compressed rf pulse is only 450 MW over 400 ns (the DLDS system proposed had 510 MW instead)
+ The klystrons have to produce a pulse of only 1.6 μs compared to 3.2 μs in the dual-moded DLDS solution
+ The energy drop due to a trip of an accelerator structure is only 0.27 GeV (0.1%) because only one of the four rf feeds per rf unit is affected

+ The total number of gate valves is reduced to about 500 compared to more than 1600 with DLDS

The disadvantages are:

– The inherent lower efficiency of the SLED-II system (75% instead of 85% for DLDS)

– The eight delay lines of 17 cm diameter have a length (29 m) that exceeds the length of the associated beam line by 3 m (optimization of the layout is under study); these delay lines have to be accommodated, either in the klystron gallery (easier) or in the tunnel (less convenient)

– The dual-moded SLED-II system has never been tested

– 4064 klystrons are required which is a relatively large number (CLIC 448, TESLA 572)

– The vacuum system has an extension of about 300 m in four branches

– The trip of one modulator reduces the energy of the beam by 1.1 GeV (0.43%)

It is planned to test the dual-moded SLED-II in NLCTA with four 50 MW klystrons of the XL4 type providing an rf pulse of the nominal length of 1.6 μs. Thus, it will be possible to produce an output pulse of 600 MW in 400 ns. This is 33% more power than the nominal power and will allow testing of the system with a good engineering margin. These tests should be completed in 2003. They are very welcome as the existing experience is only with a single-moded SLED-II and power levels lower than the nominal one. Test results are available for 270 MW over 240 ns and 480 MW over 150 ns. In addition, there are plans to install 2 PPM 75 MW klystrons later to replace the four XL4 50 MW klystrons.

There is also the interesting option to operate the klystrons with 2.4 μs pulse length which would provide a compression factor of 6 and about 600 MW instead of 450 MW in 400 ns to each string of six accelerator structures at the end of each feeder.

6.4.3.2 Upgrading Options

At present, it is proposed to do the upgrading to 1 TeV center-of-mass by completing the linacs with either the replicas of the rf components used for 0.5 TeV or, more probably, by installing improved versions of these components.

As explained before, the DLDS system remains an interesting upgrading option providing about 10% higher efficiency. Two options are available:

- A single-moded DLDS as it was considered for JLC-X
- A dual-moded DLDS as it was considered for NLC

These two options are described in Section 6.4.3.2.1 and Section 6.4.3.2.2 for completeness and as reference.

6.4.3.2.1 Single-moded DLDS The basic rf unit consists of eight 75 MW klystrons operating at 11.4 GHz, the waveguide distribution system, the Delay Line Distribution System (DLDS), and 24 90-cm traveling-wave accelerator sections. The klystrons provide an rf pulse of 1.6 μs. The function of the waveguide system is to add the eight klystron pulses, to cut the resulting 600 MW pulse into four slices in time and to distribute each 400 ns slice to one of the four rf feeds. The latter consists of a magic tee and two linear systems consisting of a waveguide and two hybrid couplers (4.8 dB and 3 dB respectively) to distribute the power to three cavities per linear branch. Thus, the basic rf unit is composed of eight klystrons feeding 24 accelerator sections. A single mode is used in all the waveguides and the ones transporting power over longer distances are circular and operate with the TE_{01} mode in order to minimize the losses.

The waveguides and the accelerator sections of each DLDS unit form a connected vacuum system. It can be isolated from the other DLDS systems by gate valves on both sides of the string of the six accelerator structures at the end of each feeder. Thus, there is a vacuum valve every 5.6 m in the beam line.

Each additional linac for the upgrading contains 234 of such rf units providing in total an additional energy gain of 250 GeV per linac. The accelerator sections pertaining to two contiguous rf units are interleaved and cover a period of 169 m length per rf unit. The schematic layout of the rf unit is shown in Figure 6.2 and of the interleaved configuration in Figure 6.3.

The advantages of this scheme are:

+ High efficiency (about 85%) with most of the losses in the rectangular waveguide components

+ Component development and system architecture for the single-moded DLDS profits from the component development done for SLED-II and the operational experience with these components

+ Compared to the dual-moded DLDS: it is more compact and has less variety of components; the rf pulse length is only 400 ns in all parts of the delay lines, which provides a better engineering margin

+ Compared to the dual-moded DLDS scheme, no increase in the klystron pulse length (1.6 μs) is required

+ Lower number of klystrons for the upgrade (3741 in total compared to 4064 in the baseline)

+ Uniform distribution of the klystrons with a periodicity of about 25 m in the service tunnel, which is an advantage in the dual deep-tunnel configuration.

+ Extensive use of vacuum valves provides vacuum isolation of the individual DLDS systems, which facilitates repair and maintenance.

+ The energy drop due to a trip of an accelerator structure is only 0.27 GeV (0.1%) because the rf power in each of the four rf feeds per rf unit can be controlled independently by proper phasing of the klystrons.

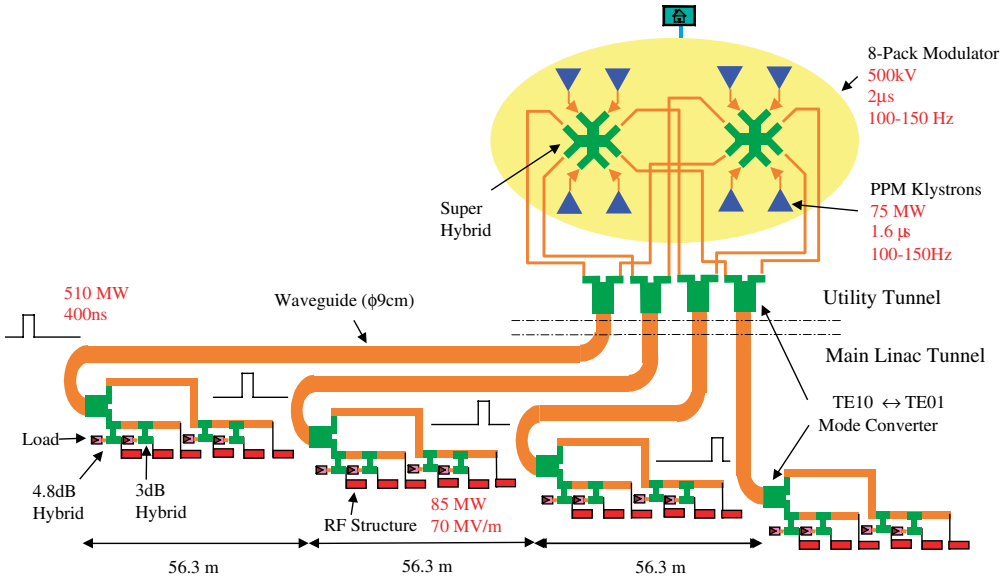

FIGURE 6.2. Schematic layout of a single-moded rf unit.

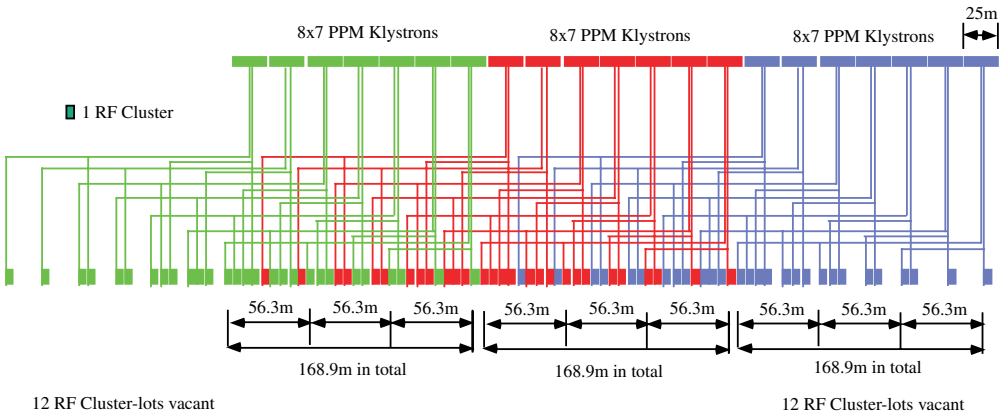

FIGURE 6.3. Interleaved single-moded DLDS scheme.

The disadvantages are:

- Waveguide components (hybrids, *etc.*) have to withstand 600 MW at 400 ns
- Interlock required against error in phase switching which could suddenly dump four times the nominal rf pulse energy into one feeder and the accelerator sections connected to it
- A high number (maximum 15) of waveguides of 3.54 inch diameter has to be accommodated in the tunnel, taking space in the tunnel cross-section
- These waveguides are not easily accessible for leak test and repair
- DLDS has no internal vacuum separation and requires waveguide flanges every 8 m
- Insertion of diagnostic sections entails irregular arrangement of DLDS
- A fully fledged power test requires a considerable amount of equipment, in particular eight klystrons and associated modulators
- Temperature effects affect the rf phasing and have to be compensated (phase measurement required)

6.4.3.2.2 Dual-moded DLDS This design is based on the assumption that 75 MW klystrons providing an rf pulse of 3.2 μs at a repetition rate of 120 Hz become available. The power distribution has the same function as in the single-moded DLDS case except that the input pulse is twice as long and is therefore cut in eight slices in time (10 ns phase switching time) in order to obtain the required 396 ns long 85 MW pulse at the input of the accelerator sections. A further difference is the use of two modes (TE_{01} and TE_{12}) in the long circular delay lines, which are needed in three out of the four main arms of one rf unit. The maximum length of an arm is 400 m. At the end of the dual-moded delay lines, the power in the TE_{01} mode flows into another, shorter TE_{10} delay line which feeds six accelerator sections via a magic tee and a linear distribution system, each feeding three sections. The power in the TE_{12} mode is converted to TE_{01} and extracted to directly feed six accelerator sections in the same configuration as described previously. Thus, each of these arms feeds 12 accelerator sections. The DLDS transmission efficiency expected is about 85%, with most of the losses occurring in the rectangular waveguide components. In total, an rf unit comprises 48 90-cm traveling-wave accelerator sections powered by only eight klystrons.

There are 117 of these rf units foreseen per 250 GeV linac. Nine 8-pack rf units (72 klystrons) are clustered together to form a nonet or a sector. The beam line length of one sector is about 470 m. There are 13 sectors per linac. Vacuum valves in the beamline separate the nonets.

The schematic layout is shown in Figure 6.4 and Figure 6.5.

The advantages of the scheme are:

+ High efficiency (about 85%) with most of the losses in the rectangular waveguide components

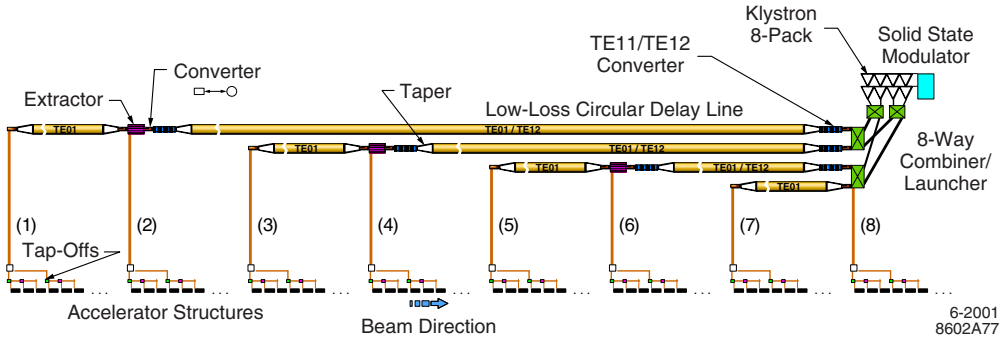

FIGURE 6.4. Schematic layout of a dual-moded rf unit.

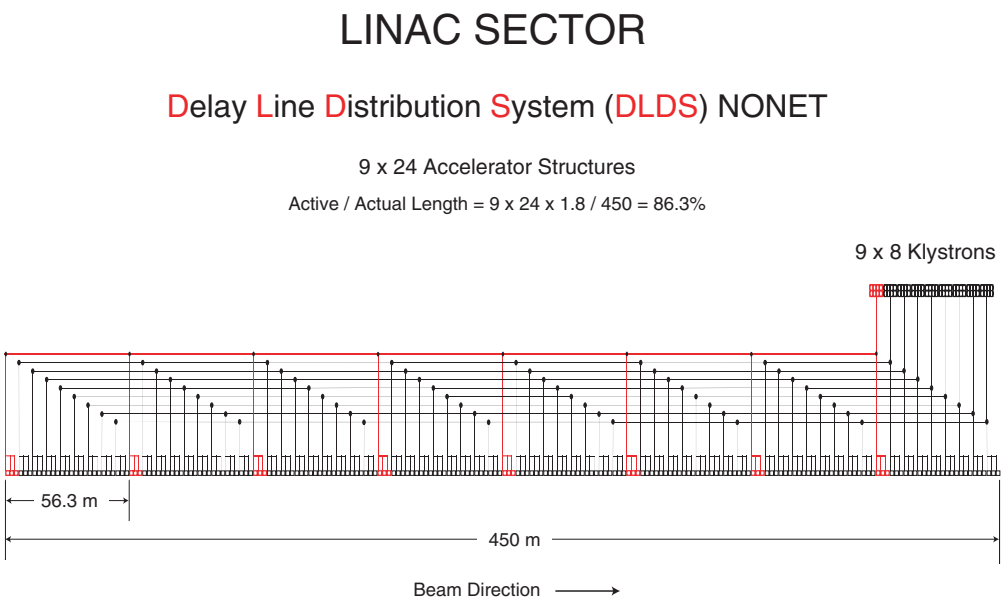

FIGURE 6.5. Interleaved dual-moded DLDS scheme.

+ Dual-mode operation of DLDS reduces the delay line length to about 60% of the single mode design
+ Number of klystrons is reduced by factor of 2 with 8 times pulse slicing, which decreases cost significantly
+ The "8-pack" clustering in nonets is particularly suitable in case the cut-and-fill method is used for the civil engineering of the klystron gallery close to the surface, resulting in a cost reduction
+ The energy drop due to a trip of an accelerator structure is only 0.27 GeV (0.1%) because the rf power in each of the eight rf feeds per rf unit can be controlled independently by proper phasing of the klystrons

In case the accelerator tunnel is deep underground, the dual tunnel layout is mandatory and the klystrons must then be distributed uniformly as done for the single-moded DLDS. However, the dual-mode delay line approach can also be applied in this case.

The disadvantages are:

– Klystron pulse is relatively long (3.2 μs), which seems to be a real challenge at 75 MW
– Testing of the full system needs a large investment since the basic unit is very large
– 48 accelerator sections drop out in case of a major fault in the rf power source (*e.g.*, modulator fault) instead of 24 for SLED-II or the single-moded DLDS version
– There are many different high-power components to design, test, and fabricate
– Components have to withstand 600 MW for 400 ns and some for 800 ns
– Very extended common vacuum system is formed by a nonet; the vacuum separation is only every 470 m on the beam line; about 1 km of 6.75 inch diameter circular waveguide have a common vacuum
– There are many waveguides in the tunnel (maximum number 36 at certain positions) which cover a significant part of the tunnel cross-section. Access to this bundle of waveguides is difficult for leak detection and repair.
– Temperature effects affect the rf phasing and have to be compensated (phase measurement required)
– An interlock is required against error in phase switching which could suddenly dump eight times the nominal rf pulse energy into one feeder and the accelerator sections connected to it

6.4.4 CLIC

CLIC operates with an rf frequency of 29.985 GHz. Since no high-power klystrons are available at this frequency, the two-beam approach has been chosen for the generation of the rf power. In contrast to the other schemes, the whole power generation system is

considered in the following as this particular approach to rf power generation is not treated in Section 6.3.

In order to produce the 130 ns long 230 MW rf pulse for each 0.5 m long accelerator section, a high-intensity electron beam, the drive beam, is decelerated in the Power Extraction and Transfer Structures (PETS) transforming kinetic energy into rf energy. Each PETS feeds two accelerator structures through very short waveguides as the drive beam runs parallel to the main beam with about 0.5 m between them. The drive beam powering one rf unit is a 39 m, 130 ns long bunch train with 2 cm spacing between the bunches. It has an initial energy of 2 GeV and is decelerated down to 0.2 GeV. At this point the beam has degraded and has to be dumped. It traverses a total of 455 PETS with a total active length of 400 m. The overall length of one unit is 624 m. Thus the basic rf unit consists of these 455 PETS and 909 TW accelerator sections. The energy gain of the main beam is 63 GeV per unit.

Note that the 30 GHz wave is induced in the PETS by the 30 GHz harmonic in the beam. This frequency is the second harmonic of 15 GHz, the fundamental frequency of the train determined by the 2 cm bunch spacing. In order to maximize the amplitude of this harmonic, the bunch must be much shorter than the rf wavelength which is 1 cm. For this reason, the rms bunch length is chosen to be 0.4 mm in the drive beam during deceleration. However, the bunch length is 2 mm in the drive-beam (linear) accelerator and combiner rings in order to limit coherent synchrotron radiation and adverse higher-order mode effects. It is shortened after the 180° bends by a bunch compressor just before the first PETS.

For 0.5 TeV in the center-of-mass (CLIC-500), four rf units per main linac are required and therefore a drive beam with four subpulses or bunch trains each 39 m long has to be produced per main linac. Each subpulse is formed by interleaving 32 bunch trains with an initial bunch spacing of 64 cm. These trains are produced by a 2 GeV normal-conducting, low-frequency (937 MHz) TW linac, the drive-beam accelerator, powered by high-efficiency long-pulse klystrons. The accelerator structures in this linac are optimized for maximum transfer of rf energy to the beam and are also fully beam-loaded in order to get highest rf to beam efficiency (97%). They operate at a fairly low loaded gradient (4 MV/m). The gun produces all the required 4×32 required bunch trains in one 17 μs long beam pulse. In each of the four subpulses, the electron bunches occupy either even or odd buckets of the drive-beam accelerator fundamental frequency, the bunches alternating between even and odd every 130 ns. Such time structure is produced after the thermionic gun in a subharmonic buncher, whose phase is rapidly switched by 180° every 130 ns. This coding of odd and even trains provides a means to separate the trains after acceleration in the linac, while keeping a constant current in the accelerator and avoiding transient beam loading.

The interleaving of the 32 trains per subpulse takes place in the following chain consisting of a delay-line combiner and two combiner rings resulting finally in four well separated subpulses with 2 cm bunch spacing. As the long pulse leaves the drive-beam accelerator, it passes through a delay-line combiner where odd and even trains are separated by a transverse rf deflector operating at 468.5 MHz. Each even bunch train is delayed in a loop of appropriate length with respect to the following odd one by 130 ns. The even and odd trains are recombined two-by-two by interleaving the trains in a second rf deflector, which results in 4×16 trains whose spacing is equal to the train length and with a bunch spacing of 32 cm in each train.

In the next stage, the trains are combined four-by-four in a first combiner ring with a 78 m circumference. It is equipped with two 937 MHz rf deflectors creating a time-dependent local deformation of the equilibrium orbit in the ring at the injection septum. After combination, the four interleaved trains having a bunch spacing of 8 cm are extracted by an ejection kicker. The whole pulse is composed of 4×4 trains. The four trains pertaining to one subpulse are combined again, using the same scheme, in a second combiner ring of 312 m circumference, yielding the required final 4 subpulses per pulse. At this point, each 2 GeV subpulse is 39 m long and consists of 1952 bunches spaced at 2 cm.

Each main linac has its own drive beam generation complex.

The advantages of the scheme are:

+ It is the only plausible technology having the potential to reach beyond 1.5 TeV center-of-mass for an e^+e^- collider, which could be already used at lower energy to get valuable experience (the baseline design is for 3 TeV)
+ Only a relatively small number of high-power klystrons is required, in total 448 in the drive-beam accelerators and four for the rf deflectors (same number for 3 TeV)
+ RF power generation is localized, which facilitates operation, repair, and maintenance
+ Upgrading of the rf power source for extension of the linacs to reach higher energies is easy because of the modular concept. It needs only lengthening of the klystron and gun pulse.
+ A single tunnel is sufficient
+ There are no active rf components in the tunnel
+ The concept allows the generation of nearly any rf frequency, the only condition being that the bunch spacing corresponds to a subharmonic of the rf
+ The drive beam generation is grouped together with the electron and positron injectors, resulting in a very compact facility where all the active high-power components, electrical power distribution, and cooling are concentrated. Access for intervention and maintenance is easy since the facility is at the surface housed in tunnels produced by cut-and-fill.

Its disadvantages are:

– One rf unit is very large, which requires a sizable investment for a fully fledged test
– The trip rate of the acceleration sections and of the PETS must be very low given the large number of these components in one rf unit, because a trip of one of these components removes one rf unit, resulting in an inadmissible energy drop of 63 GeV (25%) stopping the whole linac, at least with the present design
– A fault or failure of a critical subsystem in one of the drive-beam generation systems stops the whole main linac, which it is supposed to power
– Machine protection and beam loss control in the drive linac are very challenging

  - Four alcoves (250 m^2) are required in the tunnel per linac for the turnarounds of the subpulses and four smaller ones for the drive beam dumps (80 m^2)

A number of ideas exist about control of the field level in individual PETS and accelerator sections, which would make the requirement on the trip rate less severe, *e.g.*, tests of PETS using controllable recirculation of power have been performed in CTF2 with satisfactory results. This would allow one to control the gradients of each PETS and its associated two accelerator sections. The control of the gradients in the latter is more important as their surface fields are in the 300 MV/m range, whereas the level in the PETS is less than 100 MV/m. Such a system would limit the energy drop to 0.25 GeV (0.1%), which is acceptable for smooth operation.

The CLIC Test Facilities 1 and 2 (CTF1 and CTF2) have demonstrated the principle of the two-beam scheme. The next test facility (CTF3) will address a whole set of more advanced issues.

- Preliminary phase (2002):
  - Achieved:
    - Tests of isochronous ring with low intensity
    - Tests of deflection and funnelling, interleaving of 5 pulses in the isochronous ring
  - Planned:
    - Improved precision of interleaving and more uniform intensity in the train, test of CTF3 deflector
    - Test of photoinjector including the laser and bunch coding techniques in 2003 to decide on the front-end option
- Phase I (2004): Full beam loading in the drive-beam linac, and wakefield control in the accelerator sections of the drive linac. A special PETS for high power generation provides experience in operation and reliability of this device although parameters of the real CLIC PETS are different.
- Phase II (2005/2006): Combining techniques (funnelling with rf deflectors in a isochronous ring at higher beam intensity), experience with design of low-impedance ring and measurements of impedance, study of coherent synchrotron radiation effects

R&D work on the methods to switch off a small number of accelerator structures after a trip is mandatory but not yet planned. Work on the high efficiency modulator/klystron assemblies for the CLIC drive beam accelerator has been started. A study of the high-efficiency 937 MHz multibeam klystrons operating with a pulse length of up to 92 μs with 100 Hz has been completed indicating that a peak power of 40 MW is feasible. Note that the requirement is 50 MW peak power. Either further studies indicate a path to 50 MW or, if 40 MW is indeed confirmed, the accelerator structures of the drive beam accelerator have to be shortened and the number of rf units increased appropriately. Unfortunately, hardware development is delayed for lack of resources.

The upgrading to higher energies requires the production of more subpulses taking into account that the energy increase is quantized in steps of 0.13 TeV in the center-of-mass. Each step means lengthening of each linac by one basic unit (624 m) and of the pulse to be produced by the drive linac. The latter can be done by lengthening the PFN chains in the klystron modulators provided the original rf components were already designed for the pulse length and the average power needed in the final stage.

6.4.5 Power Efficiency

This summary given in Table 6.8, Table 6.9, Table 6.10, and Table 6.11 show the overall efficiency defined as the ratio of beam power to ac modulator input power for the schemes under consideration. The efficiency of the subsystems is also given if available. All the numbers are the nominal numbers, *i.e.*, the goals. The achieved numbers are given if available.

TABLE 6.8
TESLA 0.5 TeV

Efficiency [%]			
Goal	Achieved	Systems	Comments
85	85	Modulator	
65	65	Klystron	
94		Waveguide and circulator	
52		AC to rf	AC to rf at coupler
59		RF to beam	AC power for cryogenics/ AC power for rf=0.26
24		Overall	including power for cryogenic cooling of modules

TABLE 6.9
JLC-C 0.5 TeV

Efficiency [%]		
Goal	Achieved	Systems
67	48	Modulator
50	44	Klystron
80		Pulse compressor
24		AC to rf
26		RF to beam
6–7		Overall

TABLE 6.10
JLC-X/NLC 0.5 TeV

Efficiency [%]			
Goal	Achieved	Systems	Comments
80	50–60	Modulator	
55	60	Klystron	
75		SLED-II compression	klystron output to acc.section input
33		AC to rf	AC to acc.section input
27		RF to beam	input acc.section to beam
9		Overall	

TABLE 6.11
CLIC 0.5 TeV

Efficiency [%]		
Goal	Systems	Comments
90	Modulator	
65	Klystron	
93	Drive beam acceleration	RF input of drive linac to drive beam
82	Deceleration	Drive beam to transfer structures
95	Transfer structure	Power to transfer structures to rf output
95	Power transfer	RF output to input acc.sections
40	AC to rf	AC to acc.section input
23	RF to beam	
9	Overall	

6.4.6 Conclusions

The Working Group has examined the feasibility of each individual scheme and its subsystems taking into account the results of the R&D work done. Concerns and R&D tasks are listed here.

TESLA

Concerns and R&D:

- The proposed system for TESLA-500 is tested but a long-term test at nominal power of a number of modules has not yet been conducted. This should be planned in either TTF1 or TTF2. (Ranking 2)
- R&D is required for the upgrading to 800 GeV. Once the components are developed, they should be thoroughly tested. The proposed solutions look plausible. (Ranking 1)

JLC-C

Concern and R&D:

- Operation at full power of rf pulse compressor and, later, of a full rf unit are needed. The planned high-power tests of pulse compressor and of a full rf unit for SCSS are very welcome as well as the operation of four units for SCSS. (Ranking 1)

JLC-X/NLC

Concerns and R&D:

- Operation of a basic unit needs demonstration; in particular, tests with the nominal power level and pulse length using the new dual-moded SLED-II are required. (Ranking 2)
- The planned test of a subset (four XL4 klystrons and one dual-moded SLED-II) at nominal power in NLCTA, including the testing at higher power levels to establish an engineering margin, is currently supported at SLAC. Eventually, a complete basic unit (modulator, 8 klystrons, four dual-moded SLED-II, and all waveguide components) should be assembled and tested. (Ranking 1)

CLIC

Major concerns and R&D:

- A system is required to allow the switching-off of a small number of accelerator sections in main linac (or a requirement of excessively low trip rate of these sections and PETS). (Ranking 1)

- Machine protection for the drive-beam decelerator (beam loss control, radiation levels) is required. Conceptual studies and R&D to find solutions are strongly recommended. (Ranking 2)

Concerns and R&D:

- Generation of drive beam by fully loaded linac, delay-ring and combiner rings, should be supported at CTF3 (Ranking 1)
- Drive beam stability in intensity and phase should be tested at CTF3. Support should be provided for laser R&D (PILOT). (Ranking 2)
- The large size of one basic rf unit requires a large investment for a complete test

6.5 ACCELERATOR STRUCTURES

6.5.1 Technology for Superconducting Structures: TESLA

6.5.1.1 General Design Goals

The main goals of the TESLA international collaboration during the past decade have been to increase the achievable gradient by a factor of 4 from the 5–8 MV/m available ten years ago, and to decrease the cost per unit length of the superconducting cavities by a similar factor. Improved understanding of gradient limiting mechanisms, combined with new techniques to fabricate, treat and prepare cavities now reliably yields accelerating gradients of more than 25 MV/m. In the most recent batch, more than twenty one-meter long niobium structures yielded an average gradient over 25 MV/m during CW (continuous wave) operation. Eight 9-cell cavities, while operating with the TESLA pulse-length of one millisecond, reached gradients of 30–35 MV/m. In the TTF, the maximum average gradient achieved in a module with stable rf operation was 23 MV/m and, when operating with beam, the maximum average gradient of a module was 21 MV/m.

Having nearly met the gradient goals, the TESLA collaboration proposes to build a 500 GeV c.m. energy linear collider with a 23.8 MV/m linac gradient. An upgrade to 800 GeV c.m. energy requires operation at a gradient of 35 MV/m, which was recently achieved in CW tests of 3 electropolished nine-cell cavities, with a fourth cavity capable of a gradient of 34 MV/m.

6.5.1.2 Choice of Structure Parameters

6.5.1.2.1 Choice of Frequency The losses in a microwave cavity are proportional to the product of conductor area and surface resistance. For a given length of a multicell resonator, the area scales with 1/f while from BCS (Bardeen, Cooper, Schrieffer) theory the superconducting surface resistance scales as f^2. In practice, there is always a residual surface resistance for a non-ideal surface, which is assumed to be independent of frequency. At an operating temperature T=2 K, it is found that the BCS resistance dominates above 3 GHz and hence the losses grow linearly with frequency. For frequencies below 300 MHz,

the residual resistance dominates and the losses scale as 1/f. To minimize the dissipation in the cavity wall one should therefore select f in the range 300 MHz to 3 GHz. Cavities in the 350 to 500 MHz regime are in use in electron-positron storage rings. Their large size is advantageous to suppress wakefield effects and higher-order mode losses. However, for a linac of several 10 km length the niobium and cryostat costs for these bulky cavities would be prohibitive, hence a higher frequency has to be chosen. Considering material costs, f=3 GHz might appear the optimum, but there are compelling arguments for choosing about half this frequency:

- The wakefield losses scale with the second and third power of the frequency ($W_{long} \sim f^2$, $W_{trans} \sim f^3$). Beam emittance growth and beam-induced cryogenic losses are therefore much higher at 3 GHz.
- The f^2 dependence of the BCS resistance sets an upper limit of about 30 MV/m at 3 GHz. Hence, choosing this frequency would definitely preclude a possible upgrade of TESLA to 35–40 MV/m. The choice for 1.3 GHz was motivated by the availability of high power klystrons.
- For cost optimization a cavity length of at least 1 m is desirable. For 3 GHz the number of cells would be larger. Hence the problem of trapped modes and field flatness would be a more serious issue.

Niobium film cavities have also been studied in detail by a CERN group at 1.5 GHz [30], but compared to bulk niobium cavities, they do not reach the same performance.

6.5.1.2.2 Cavity Geometry A multicell resonator is indispensable for maximizing the active acceleration length in a linac of several 100 GeV. With the increasing number of cells per cavity, however, difficulties arise from trapped modes and uneven field distribution in the cells. The design of the cell shape was guided by the following considerations:

- The cell shape is azimuthally symmetric with an ellipsoidal longitudinal profile
- A large iris radius is chosen to reduce wakefield effects

For the TESLA cavities, R_{iris}=35 mm was chosen, leading to a cell-to-cell coupling of 1.87% and a ratio of peak field on the iris to accelerating field of E_{peak}/E_{acc}=2. The contour of a half-cell is composed of a circular arc around the equator region and an elliptical section near the iris.

The half-cells at the end of the 9-cell resonator have a slightly different shape to ensure equal field amplitudes in all 9 cells. In addition, there is a slight asymmetry between the left and right end cell, which prevents trapping of higher-order modes.

6.5.1.2.3 Number of Cells The reference design is a 9-cell structure which was the optimum for cost efficiency and technical feasibility. With more than 9 cells the desired field flatness of more than 98% is difficult to achieve.

The proposed 2 × 9 cell superstructure increases the filling factor by about 6% and reduces the number of power couplers and other rf components by a factor of 2 as well as the number of flange connections. The field flatness can be achieved with a frequency tuner on each of the substructures. HOM damping is achieved with the same principle as in the reference design. This concept was tested with beam in late 2002, in a 2 × 7 prototype superstructure.

6.5.1.2.4 Active Tuning The electromagnetic fields exert a force on the currents induced in a thin surface layer leading to a deformation of the cavity and a frequency shift. In the present TTF cavities this shift amounts to 250 Hz at 25 MV/m during the 1 ms long beam pulse.

For TESLA-800 an active piezoelectric tuner is foreseen to compensate the detuning during each rf pulse. In a test at 24 MV/m the detuning was fully compensated. With the piezoelectric frequency stabilization the cavities can be operated at 35 MV/m with the rf power overhead of 10% while an overhead of 40% would be needed without piezo compensation.

Tests on the pulsed operation of piezo crystals at liquid helium temperatures in a radiation environment are underway. There will be further tests on cavities in 2003. The incorporation of the piezos into the tuning mechanism is underway.

6.5.1.3 HOM Damping

The intense electron bunches excite higher order eigenmodes (HOMs) in the resonator whose energy must be coupled out to avoid multibunch instabilities and beam breakup. This is accomplished by HOM couplers mounted on the beam pipe sections. The HOM couplers are mounted at both ends of the cavity with a nearly perpendicular orientation to ensure damping of dipole modes of either polarization. A 1.3 GHz notch filter is incorporated to prevent energy extraction from the accelerating mode.

A problem arises from trapped modes which are concentrated in the center cells and have a low field amplitude in the end cells. An example is the TE_{121} mode. By an asymmetric shaping of the end half-cells, the field amplitude of the TE_{121} mode is enhanced in one end-cell while preserving the field homogeneity of the fundamental mode. The two polarization states of dipole modes would, in principle, require two orthogonal HOM couplers on each side of the cavity. In a string of cavities, the task of the orthogonal HOM coupler can be taken over by the HOM coupler of the neighboring cavity. The viability of this idea was verified in measurements.

In experimental tests on 9-cell structures, it was verified that all HOMs, which couple strongly to the beam (high R/Q), were damped with the exception of one mode at 2.58 GHz. This effect has by now been well understood and good damping can be restored by a re-orientation of one of the HOM couplers. Very high frequency modes will be absorbed by a high loss material at a temperature level of 70 K inserted into the beam pipe between cryomodules to avoid additional heat load into the helium at 2 K.

6.5.1.4 Fabrication and Assembly

The superconducting resonators are fabricated from 2.8 mm thick niobium sheets by electron-beam (EB) welding of deep-drawn half-cells. The tubes for the beam pipes and the coupler ports are made by back extrusion and are joined to the cavity by EB welds.

6.5.1.4.1 Niobium Specification The most important metallic impurity in niobium is tantalum, with a typical concentration of 500 ppm. The interstitially dissolved gases (mainly oxygen) act as scattering centers for the unpaired electrons and reduce the thermal conductivity at 2 K. The niobium ingot is outgassed by several melting cycles in a high vacuum electron beam furnace. The interstitial oxygen, nitrogen and carbon contamination is reduced to a few ppm. The Nb ingots are forged and rolled into sheets of 2.8 mm thickness. After rolling, the Nb sheets are first degreased and cleaned by chemical etching. The sheets are then annealed for 2 hours at 700–800°C in a vacuum oven at 10^{-6} mbar to achieve full recrystallization and a uniform grain size of about 50 μm.

The niobium sheets for the last two cavity production series were all eddy-current scanned to eliminate material with tantalum or other foreign inclusions before the deep drawing of half cells. More than 95% of the sheets were found free of defects; the remaining ones showed grinding marks, imprints from rolling or large electrical signals due to small iron chips. Most of the rejected sheets were recoverable by applying some chemical etching. The eddy-current check has proven to be an important quality control procedure, not only for the cavity manufacturer but also for the supplier of the niobium sheets.

6.5.1.4.2 Cavity Fabrication Cavity fabrication is a delicate procedure, requiring intermediate cleaning steps and a careful choice of the weld parameters to achieve full penetration of the joints. First, two half cells are connected at the iris; the stiffening rings are welded in next. At this point weld shrinkage may lead to a slight distortion of the cell shape which needs to be corrected. Particularly critical are the equator welds which are made from the outside. A reliable method for obtaining a smooth weld seam at the inner cavity surface is to apply 50% of the power to the first weld pass, and 100% on the second. A slightly defocused electron beam rastered in an elliptic pattern is used.

The electron-beam welding technique of niobium cavities has been perfected in industry to such an extent that the weld seams do not limit cavity performance below 30 MV/m.

Stringent requirements are imposed on the weld preparation to prevent the degraded performance at the equator welds encountered in the first production series of TESLA cavities. After mechanical trimming, the weld regions are cleaned by a light chemical etching followed by ultra-pure water rinsing and clean-room drying. The cleaning process is performed not more than 8 hours in advance of the EB welding.

The challenge for a welded construction is the tight mechanical and electrical tolerances. These can be maintained by a combination of mechanical and radio frequency measurements on half cells and by careful tracking of weld shrinkage (see below). The procedures established during the TTF cavity fabrication are suitable for large series production, requiring quality assurance measurements only on a small sample of cavities. The cavities are equipped with niobium-titanium flanges at the beam pipes and the coupler ports. NbTi can be electron-beam welded to niobium and possesses a surface hardness

equivalent to that of standard UHV flange material (stainless steel 316 LN/DIN 1.4429). Contrary to pure niobium, the alloy NbTi (ratio 45/55 by weight) shows no softening after the heat treatment at 1400°C and only a moderate crystal growth. O-ring type aluminum gaskets provide reliable seals even in superfluid helium, which is only needed for the vertical CW acceptance test.

After implementation of the additional quality control measures (eddy-current scanning, etching and cleaning the weld regions), no foreign material inclusions nor weld contaminations have been found in new cavities tested so far. Three companies have been qualified for the cavity fabrication.

6.5.1.4.3 Fabrication Tolerances The tolerances on cavity fabrication are described in Table 6.12.

TABLE 6.12
Tolerances on cavity fabrication.

Cavity length [mm]	±3
RF frequency [MHz]	±0.1
Field flatness [%]	98

These specifications have been met in the second and third production series of the TTF cavities after the following checks on the fabrication process were introduced:

- Frequency measurement on all half cells
- Contour measurement on selected half cells
- Frequency measurement on selected dumb-bells
- Frequency measurement on all dumb-bells after welding of the stiffening ring

6.5.1.4.4 Alternative Fabrication Methods The standard fabrication by deep-drawing and electron-beam welding is a proven and cost-efficient technology. It has been demonstrated that it is industrially feasible. There exist alternative fabrication techniques: spinning and hydroforming. Both techniques have shown very good performance in one-cell cavities resulting in gradients above 38 MV/m (spun) and 41 MV/m (hydroforming) respectively. The fabrication of multicell cavities is underway. Tests are expected to take place in 2002.

6.5.1.4.5 Post-Fabrication Treatment A layer of 100–200 μm is removed in several steps from the inner cavity surface to obtain good rf performance in the superconducting state. The standard method applied at DESY is called Buffered Chemical Polishing (BCP), and uses an acid mixture of HF (48%), HNO_3 (65%) and H_3PO_4 (85%) in the ratio 1:1:2. The acid is cooled to 5°C and pumped through the cavity in a closed loop. After rinsing

with ultra-pure water and drying in a class 100 clean room, the cavities are annealed at 800°C in an Ultra High Vacuum (UHV) oven to out-gas dissolved hydrogen and relieve mechanical stress in the deep drawn niobium. In a second UHV oven the cavities are heated to 1300–1400°C at which temperature the other dissolved gases diffuse out of the material, and the residual resistivity ratio RRR increases by about a factor of 2 to around 500. To absorb the oxygen diffusing out of the niobium and to prevent oxidation by the residual gas in the oven (pressure $<10^{-7}$ mbar), a thin titanium layer is evaporated on the inner and outer cavity surface (Ti being a stronger getter than Nb). The titanium layer is later removed by 80 μm and 20 μm BCP of the inner and outer cavity surface respectively. This high-temperature treatment with Ti getter is referred to as post-purification. A severe drawback of post-purification is the considerable grain growth of the niobium: post-purified cavities are vulnerable to plastic deformation and have to be handled with great care. After the final heat treatment, the cavities are mechanically tuned to adjust the resonance frequency to the design value and to obtain equal field amplitudes in all 9 cells. This is followed by a light BCP, three steps of high-pressure water rinsing (100 bar), and drying in a class 10 clean room. The final acceptance step is an rf test in a superfluid helium bath cryostat.

6.5.1.4.6 Industrialization The manufacturing process of all TTF cavities has been done in industry. There exists a detailed specification for the niobium material as well as for the cavity fabrication so that very reproducible performance can be achieved. This has been demonstrated in the last two cavity production series.

All the chemical treatment steps can be done in industry. Chemical etching of niobium cavities is a standard procedure which has been used at CEBAF, LEP and also for cavities in synchrotron radiation storage rings.

Studies have been conducted by industrial companies showing the industrial feasibility of the cavity processing and serve as a solid basis for the cost estimate.

6.5.1.5 Structure Environment

6.5.1.5.1 Cryomodule Each 9-cell cavity is equipped with its own titanium helium tank, a tuning system driven by a stepping motor, a coaxial rf power coupler capable of transmitting more than 400 kW, a pickup probe, and two higher-order mode (HOM) couplers. To reduce the cost for cryogenic installations, 12 cavities and a superconducting quadrupole are mounted in a common vacuum vessel and constitute the cryomodule. Within the module the cavities are joined by stainless steel bellows and flanges with metallic gaskets. The cavities are attached to a rigid 300 mm diameter helium supply tube which provides positional accuracy of the cavity axes of better than 0.3 mm. Invar rods ensure that the distance between adjacent cavities remains constant during cooldown. Radiation shields at 5 and 60 K together with 30 layers of superinsulation limit the static heat load at the 2 K level to less than 3 W for the 17 m long module. The design of the cryomodules is advanced and suitable for industrial production.

The cavities are cooled to 2 K to achieve a high quality factor of more than 10^{10} (5×10^{9}) at 23.8 MV/m (35 MV/m). The pressure drop in the Helium supply line for TESLA in the most unfavorable case (3.8 km) is 0.94 mbar causing a temperature difference of

about 0.1 K. For stable cavity operation, it is desirable to have pressure fluctuations of less than 1 mbar.

6.5.1.5.2 Cryoplant Superconducting technology has been used in many circular accelerators such as LEP, TRISTAN, Tevatron and HERA, and many new projects either under construction (LHC, JHF, SNS) or in the planning stage have adopted this technology in their design. That proves that cryotechnology is rather mature and commonly available. The TESLA cryosystem design was based on the experience at CERN for the LHC cryosystem. These studies, including the layout of the TESLA cryoplants, have been carried out in close collaboration with industry. All major components for the TESLA cryogenics have been successfully used for years in similar plants. HERA experience already shows that an availability of the cryosystem of greater than 98% can be achieved.

6.5.1.5.3 Couplers For the coaxial power coupler an elaborate two-window solution was chosen for optimum protection of the cavity against contamination during mounting in the cryomodule and against window fracture during linac operation. The coaxial couplers consist of a "cold section" which is mounted on the cavity in the clean room and closed by a ceramic window, and a "warm section" which contains the transition from the coaxial line to the waveguide. This part is evacuated and sealed against the air-filled waveguide (WR 650) by a second ceramic window.

Couplers have been limiting elements of superconducting cavities in the past. The first series of TESLA high power input couplers have been the limit for one module assembled for the TTF linac. After a few months at lower power levels (corresponding to 15 MV/m) in the machine the power could not be raised without new conditioning. The major change in the new series of couplers tested in the recent module run was to implement a bias voltage between inner and outer conductor to suppress multipacting. This concept has already been used with success for the power couplers for the superconducting cavities in LEP.

The biased couplers have performed up to 2 MW at 1.3 ms in a traveling-wave mode in warm test stands. In the horizontal test stand several cavities have run with these couplers above 30 MV/m without beam. For these couplers no new conditioning was needed after running the linac at lower gradients and the power could be raised within one shift.

6.5.1.6 Gradient Limitations

6.5.1.6.1 Status for TESLA-500 The most recent TTF cavities exceed the 23.8 MV/m operating gradient of TESLA-500. The last production series with the standard BCP achieves an accelerating gradient of 26.1±2.3 MV/m at Q=10^{10}.

After having passed the acceptance test in the vertical bath cryostat, the cavities are welded into their liquid helium container and equipped with the main power coupler. The accelerating fields achieved in the vertical and the horizontal test are well correlated. Only in rare cases was a reduced performance seen, usually caused by field emission. Several cavities improved their performance in the horizontal test because of operation with short (millisecond) pulses instead of the continuous wave (CW) operation in the vertical cryostat. The results show that good performance of the cavities can be preserved if great care is taken to avoid dust contamination during mounting of the helium vessel and power coupler.

In one of the cryomodules installed in the TTF linac, the maximum usable gradients were measured for each of the eight cavities. The average gradient was 22.7 MV/m, indicating that installation of the individual cavities into a module does not degrade their performance. A long-term test at maximum gradient is underway.

The typical processing times for the high power couplers and cavities are a few days. Recently, the use of preconditioned couplers has shown to reduce the conditioning time significantly to about a day. A viable alternative is to coat the couplers with a thin TiN layer, A TiN coated coupler has shown the same time processing as a pre-processed coupler.

6.5.1.6.2 Status of R&D for TESLA-800 For further performance improvement, the most promising method today for surface preparation is electropolishing. The Buffered Chemical Polishing (BCP) used at TTF to remove a 100–200 μm thick damage layer produces a rough niobium surface with strong grain boundary etching. An alternative method is electropolishing (EP) in which the material is removed in an acid mixture under current flow. Sharp edges and burrs are smoothed out and a very glossy surface can be obtained. The electrolyte is a mixture of H_2SO_4 (95%) and HF (46%) in a volume ratio of 9:1. The bath temperature is 30–40°C. The process consists of two alternating steps: oxidation of the niobium surface by the sulphuric acid under current flow (current density about 500 A/m^2), and dissolution of the Nb_2O_5 by the hydrofluoric acid. The material removal is around 40 μm per hour.

Results on single-cell cavities at KEK and from a collaboration of CERN-CEA-DESY demonstrate that electropolishing is the superior surface treatment method. Accelerating gradients of 35–42 MV/m have been achieved in more than a dozen single-cell resonators. This includes electron-beam welded as well as hydroformed and spun cavities. Recently it has been found that an *in-situ* baking of the evacuated cavity at 100–150°C, following EP and clean water rinsing, is an essential prerequisite for reaching the highest gradients without a strong degradation in quality factor. This baking was applied to all single-cell cavities and yielded reproducible results. Several surface analytical studies have been done and the effect is linked to the diffusion of impurities (most notably oxygen). A program of measuring the basic properties of the *in-situ* baked niobium used in the cavities is pursued at the same time.

The transfer of the electropolishing method to multicell cavities has been studied at KEK for some years. Electropolishing has been used by Nomura Plating for KEK's cavities for many years (*e.g.*, Tristan, KEK-B). In a collaboration of KEK and DESY the electropolishing of TESLA nine-cell cavities is being studied. In a first test a 9-cell resonator from the first production series (the niobium material of this production series was not eddy-current scanned) has been electropolished by Nomura Plating, improving its performance from 22–32 MV/m. More recently, three electropolished cavities from the last production series achieved the performance needed for TESLA-800 in a CW measurement: 35 MV/m at a Q_0 larger than 5×10^9. The cavities were tested for several hours at CW. A fourth cavity of this batch achieved 34 MV/m. Another four cavities will be electropolished at KEK and tested at DESY in 2002. To further study the EP technique of multicell cavities, DESY is setting up an electropolishing facility for 9-cell and 2×9 superstructure cavities.

6.5.1.6.3 Dark Current Dark Current measurements at the TTF linac have shown that the threshold gradient is typically 1 MV/m below the maximum gradient as determined in the vertical test. Two accelerator sections with eight cavities each were studied. In both cases one single cavity produced most of the dark current. At high gradient (20.8 MV/m in module 3) a current of up to 100 nA was measured. Detuning of the particular bad cavity reduced the dark current for the remaining seven cavities to approximately 30 nA. Up to the highest possible gradient, the measured dark current showed a pure Fowler-Nordheim behavior. Signals were measured on beam axis using Faraday-cup like devices as well as Compton diodes. This *in-situ* measurement takes into account both the dark current emitted in the individual cavities and the capture probability in the presence of the neighboring cavities. Even though the first dark current measurements at gradients close to the limiting gradient meet TESLA requirements, on-going measurements will give more results for the next accelerator sections. A more quantitative dark current measurement during the vertical cavity tests could improve the understanding of gradient limitations during operation.

6.5.1.6.4 Superstructure A fundamental design goal for a linear collider is to minimize the cost of the accelerator while maximizing the active acceleration length. Hence, it is desirable to use accelerator structures with as many cells as possible, both to reduce the number of couplers and waveguide components and to increase the filling factor. However, the number of cells per cavity (N) is limited by the conditions of field homogeneity and the presence of trapped modes. The sensitivity of the field pattern to small perturbations grows quadratically with the number of cells. The probability of trapping higher-order modes within a structure also increases with N, and such modes with a small field amplitude in the end cells are difficult to extract by the HOM couplers.

The limitations on the number of cells per cavity can be circumvented by joining several multicell cavities to form a so-called superstructure. Short tubes of sufficient diameter (114 mm) enable power flow from one cavity to the next. The chain of cavities is powered by a single input coupler mounted at one end. HOM couplers are located at the interconnections and at the ends. All cavities are equipped with their own tuners. The cell-to-cell coupling is 1.9%, while the coupling between two adjacent cavities in a superstructure is two orders of magnitude smaller at 3×10^{-4}. Because of this comparatively weak inter-cavity coupling the issues of field homogeneity and HOM damping are much less of a problem than in a single long cavity with N=18 cells. The shape of the center cells is identical to those in the 9-cell TTF structures while the end-cells have been redesigned to accommodate the larger aperture of the beam tube. The cavities are tuned to equal field amplitude in all cells and are then welded into their liquid helium tanks and joined to form the superstructure. It has been verified that the pre-tuning of the cavities can be preserved during the assembly steps.

The main concerns for a chain of cavities fed by a single input coupler is the flow of the rf power through the interconnecting beam pipes, and the time needed to reach equal field amplitude in all cells during pulsed-mode operation. The power flow has been extensively studied with two independent codes, HOMDYN and MAFIA. The relative spread in energy gain in a train of 2820 bunches is predicted to be less than 10^{-4}, indicating that the energy flow is sufficient to refill the cells in the time interval between two adjacent bunches.

The 2 × 9 cell superstructure under consideration improves the filling factor by 6% and requires a factor of 2 fewer main power couplers in the machine, which is an important cost factor. The combination of two 9-cell resonators achieves a high filling factor of 85% and is 2.39 m long. This structure can be (electro-)chemically treated and handled with an upgraded version of the facilities at TTF. Keeping the total length of the collider constant, the superstructure allows to reach the 500 GeV c.m. energy with a gradient of 22 MV/m, compared to 23.8 MV/m with individual 9-cell cavities. In the superstructure the main power coupler must transmit 437 kW of traveling wave power at 500 GeV c.m. energy and 705 kW at 800 GeV. The TTF couplers have been tested up to 1500 kW and should be sufficient to feed the superstructure. To provide an additional safety margin for the operation at 35 MV/m (TESLA-800) the diameter of the cold coupler section will be increased from 40 mm to 60 mm. The higher-order modes have been extensively studied for the superstructure. Nearly all modes propagate through the 114 mm diameter beam pipe and are efficiently damped with 4 HOM couplers mounted at the interconnection and at both end tubes. The details of the dipole mode impedances differ somewhat from the 9-cell cavity, but the overall effect on the beam dynamics is similar.

Two 2 × 7 cell niobium prototypes are undergoing a beam test in the TTF linac. In these prototypes the 7-cell cavities are joined by welding. The third generation of TTF input coupler and three HOM couplers are used. The beam test will help verify the energy spread computations and the rf measurements on the copper models. In addition the performance of the HOM couplers, which are exposed to a higher magnetic field due to the enlarged beam tube diameter, can be tested. Preliminary results from rf measurements show that the tuning of the structure and the damping of the HOMs works as expected.

6.5.1.7 Superconducting Cavity Operating Experience

6.5.1.7.1 Background Superconducting cavities behave differently from normal conducting structures in that their maximum operating gradient is set by cavity quench, field emission, or Q degradation- not under normal circumstances by structure breakdown. If quenches have not limited operation at a lower gradient, then field emission and Q degradation (below the allowed Q_0) set the maximum operating gradient of a cavity. This maximum gradient is not a hard limit. It results in high cryogenic load, radiation, and dark current from particular cavities, but does not trip off cavities. If observed to increase during operation, then the gradient of particular cavities can be lowered.

A cavity quench can trip off cavities, but it is a thermal process, not a breakdown or discharge. Therefore it is not the dramatic event that occurs in superconducting magnet systems because the stored energy is very limited. The time constant of development of the quench depends on the power supplied. If a lot of excess power is supplied, then the quench develops rapidly. If one is at the threshold, then the quench develops slowly (100 μs to 1 ms). This slow growth of a normal zone can be detected in a decrease of gradient in a cavity with constant input power. This information can be used to inhibit rf power part way through the pulse (a soft inhibit). Additionally the gradient can be slightly reduced on subsequent pulses until a stable gradient level is reached. A complete shutoff of the rf station is not necessary. However, in some cases hard inhibits may occur. Those can be handled by detuning the frequency of the cavity that trips off. After detuning the rf station can be switched on again.

There is one other situation where a breakdown in a superconducting cavity can behave like breakdown in a copper cavity. This is the situation for High Peak Power Processing (HPPP). HPPP is used to improve cavity performance. As input power as high as possible is applied to the cavity for short pulses (∼1/2 ms), emitter sites can be blown up before the quench has time to develop. The result is a crater on the Nb surface, and, when successful, destruction of the emitter and higher gradient performance. This is not a standard procedure during beam operation.

Performance can also be limited by the input coupler. Input couplers can be limited by multipacting, electron emission, vacuum increase and breakdown at the windows much as in normal conducting cavities. The couplers are rf processed off line prior to installation on the cavities. Then they are processed for a short time on the cavities, both warm and cold.

6.5.1.7.2 Observations and Operating Experience When trying to extrapolate to the operation of 20000 cavities of the collider, there is to date limited experience on what makes cavities trip and just how often. Emphasis has been placed on other more pressing operational issues rather than on the accumulation of statistics of cavity trips under long-term stable conditions. Our basic impression is that cavity operation is very stable by itself when other disturbances are not present. This section outlines some of the experience.

Vertical Dewar Tests After chemical preparation the bare cavities are mounted in a dewar for initial measurements of Q versus E and maximum gradient attainable. These are CW measurements, and though there are a few processing events, this is not a processing activity but rather a measurement of the cavity performance. Because it is CW, the test time can reflect considerable effective pulse operation time for the bare niobium cavity. The time at CW operation is limited by the cryogenic system that supplies the vertical dewar (the system is different from that supplying the modules).

CHECHIA Tests CHECHIA is a horizontal test cryostat. Fully dressed cavities including power input coupler, helium vessel and tuner are tested here. These tests are with pulsed rf like in final operation (without beam). The achievable gradient is again measured, and cryogenic measurements are made to determine the cavity Q. Often the limiting gradient is higher than in the vertical CW test because of the pulse length and duty factor. A relevant observation during these tests is that to carry out the Q measurement the cavity must operate without any trips for a few hours. Measurements are done at a number of gradient values, each taking one hour. If anything happens to stop the measurement (trip), then the measurement must start over. As this is standard procedure on all cavities tested in CHECHIA, we can assume that the trip rate is low relative to one event per hour. The couplers of the last series with bias voltage have been run to gradients of more than 30 MV/m. Testing time in CHECHIA could be extended but would need to go to about a day or two in order to be meaningful for extrapolation to linear collider klystron up time estimates and energy reduction from trips and their recovery.[1]

[1] If the measurement results in 1 trip per cavity in 30 hr, with an arbitrary choice of a 1/2 minute recovery time, then an average of three klystrons would be down per linac. This corresponds to an energy reduction, on average, of one percent (one percent is within the TESLA energy budget).

ACC1 Test 2002 In April-May 2002, one eight-cavity module (ACC1, Mod3) has been run at high gradient and long pulse.[2] The main goals of this run were to exercise the module at near its maximum gradient and to accelerate long bunch trains. The run was carried out under dynamic conditions with beam tuning going on and various levels of operator expertise. Data analysis is still in progress.

Some of the preliminary results are given here. Seven of the eight cavities were operated at gradients between 19 and 22 MV/m. The overall average gradient was between 19.5 and 21 MV/m (as measured with the beam). Typical module on time was ∼90%. Trips have been counted but their source has not been investigated. Over a total of 42 days, 291 trip events were recorded, an average of 8.4 events/day at 5 Hz for the 8-cavity module (when corrected for operating part of the time at 1 Hz). This trip rate includes amongst other things both cavity and coupler trips. Partway through the run time, a soft rf inhibit was implemented so that potential quenches could be detected without tripping the interlock system.

Although this run cannot be extrapolated to determine the collider linac operational reliability, we believe these experiences are positive and point out some of the basic differences between superconducting and normal conducting cavity operation. We also believe that a sophisticated and flexible low-level rf system will be needed to handle a variety of exceptions. We note as well that the cavities in this test have been in operation for over 12000 hr at lower gradients. There was no need for reprocessing them to get back to the maximum value. For this run they were operated very close to their limit, a situation that will not occur for the 500 GeV collider.

For the couplers no reconditioning was needed for the ACC1 run. The couplers of this module are equipped with a bias voltage that can be used to suppress multipacting.

The couplers from the first series without bias voltage on the other accelerating module in the linac limit the cavities to a gradient of 15 MV/m. Reconditioning of these couplers was not performed due to the limited time.

6.5.1.8 Potential for Upgrading to Gradients Above 35 MV/m

Theoretical arguments [31] indicate that the critical magnetic field for rf is the superheating field, which is about 230 mT for niobium at 2 K. Using 4.26 mT/(MV/m) for the TESLA structure, this translates into a limiting gradient of 54 MV/m. The highest value for the rf critical field at 2 K measured to date [31] is 175 mT, corresponding to a gradient of 41 MV/m. However, it can be argued that this lower measured value was due to heating at surface imperfections, and that with further improvements in surface quality critical fields closer to the theoretical limit will be obtained [32]. Improvements in structure design could also, in principle, marginally increase the limiting gradient. Thus it seems reasonable that gradients on the order of 50 MV/m might eventually be achieved with niobium.

There is the possibility of using other Type II superconductors for the cavity surface, such as Nb_3Sn (T_c=18.2 K, B_c=535 mT). This material has already been investigated in the hope that, because of the high value for T_c, high Q's could be obtained at 4.2 K. So far, however, the measured value for the surface conductance at 4.2 K has fallen well below the

[2] This module was built up in 1999. Three more modules have been built and are awaiting the performance test in the Linac at the end of 2002.

theoretical value [32]. Other materials, such as Al Nb_3, Si V_3 and alloys in the Al_x Ge_y Nb_z family, have transition temperatures and critical fields comparable to or greater than that of Nb_3Sn. Although results to date for investigations of alternative materials have not been encouraging, it seems reasonable to support a continuing low level program of research into these materials (perhaps in a university setting) because of the potentially high payoff.

6.5.2 Technology for Normal Conducting Structures

6.5.2.1 Introduction

6.5.2.1.1 Normal Conducting Versus Superconducting The possibility of building a linear collider in the 1 TeV c.m. energy range began to be taken seriously at SLAC in the late 1970s. In order to reach an energy of this magnitude in a reasonable length, it was clear that the accelerating gradient would have to be considerably higher than that of the SLAC linac, which was then about 12 MV/m. There was no thought of using superconducting technology, since at that time the highest gradient (limited by rf breakdown) achieved in any cavity geometry approaching a practical accelerator structure was about half the modest SLAC gradient (which was limited only by klystron power). At the SLAC S-band frequency of 2.856 GHz, accelerating gradients approaching 30 MV/m were, in fact, being attained at linacs elsewhere. Consequently, it was assumed that a future high-gradient linear collider would need to be based on normal-conducting, copper structures.

The largest application of normal-conducting rf accelerator structures then (as now) was the 3-km long SLAC linac itself. Since its initial operation in 1966, the linac has been continuously upgraded for higher energy, higher intensity and lower beam emittance. Many linear accelerators built for physics research or for industrial and medical applications have been based on SLAC linac technology. As the SLC (SLAC Linear Collider) came on line, much experience directly relevant to an S-band linear collider was obtained. However, a 1 TeV linear collider operating at the SLAC gradient would have to have an active length of at least 50–60 km. Thus there was a clear challenge to develop rf technology that would make the machine shorter, and most importantly, affordable. To meet this challenge, it was equally clear from fundamental scaling laws that the operating frequency would have to be higher than S-band.

6.5.2.1.2 Choice of Operating Frequency The choice of an operating frequency has profound consequences for almost every aspect of linear collider design. The broad reasons for the frequency choice for each design are given in the Overview sections. It is useful to expand on this discussion by focusing on the rf technology underlying these frequency choices.

At SLAC during the 1980s, frequencies ranging from S-band to 17 GHz were given serious consideration in various paper designs. In 1986, motivated in part by the nascent work at CERN on a site-filling TeV linear collider, it was decided it was time to cut metal and build both a prototype klystron and pulse compression system. An X-band frequency was chosen as a compromise between the drive for high gradient, the difficulty of building a klystron at a higher frequency, and the cost and availability of rf components (medical radiation therapy accelerators already existed at X-band). The exact frequency of 11.424 GHz was chosen to be a multiple of the SLAC linac frequency. The JLC-X project later adopted the

same frequency, making possible a close collaboration between the two laboratories on almost all aspects of the technology of a high-energy linear collider. The JLC-X/NLC group believes that the choice of an X-band frequency gains the major cost benefits of a high frequency rf system, while still allowing achievable alignment tolerances associated with stronger wakefields. Until recently, the design was based on unloaded/loaded gradients of 70/55 MV/m; with the adoption of the SLED II pulse compression system, the values are now 65/50 MV/m.

The CLIC group at CERN proposes a novel two-beam accelerator aimed at multi-TeV energies. This concept allows for high frequency since it does not rely on conventional rf sources, which become progressively limited in output power with increasing frequency. A frequency of 30 GHz was chosen because it gives a high "transformer ratio" (the gradient is related to the linac/drive beam frequency ratio). Also, this frequency was considered to be close to the limit beyond which standard technology for the fabrication of copper structures can no longer be used. The high frequency for the CLIC design makes it possible to keep the rf energy required per pulse at a reasonable level for a loaded gradient as high as 150 MV/m. However, the small beam aperture of the accelerator structure puts stringent requirements on wakefield control.

The JLC-C design proposes a frequency of 5.7 GHz, with unloaded/loaded gradients of 44/34 MV/m. By choosing a frequency midway between S-band and X-band, the design approach is to achieve a reasonably high gradient while exploiting the advantages of more conventional lower frequency technology. For example, klystrons are easier to build and pulse compression is achieved using a simple high-Q energy storage cavity rather than an expensive system of long delay line pipes.

6.5.2.1.3 Implications of Frequency Choice for Structure Design With the large variation in the proposed operating frequencies, one might wonder if there is indeed an optimal frequency. In examining the design choices for these proposals, one instead sees that with increasing frequency there is a general tradeoff of potential cost savings versus increasing operational difficulty. On the plus side, higher frequency affords shorter structure filling times, shorter bunch trains lengths (typically several times the fill time) and higher structure shunt impedance. With higher impedance, reasonably good rf-to-beam efficiencies are achievable at higher gradients, which makes the linac shorter. With a shorter linac and bunch train length, less rf energy per pulse is required, which decreases the number of power sources. Opposing this trend is the increasing cost of rf energy with frequency (the CLIC approach circumvents this limitation by using low frequency klystrons to accelerate drive beams that are compressed and de-accelerated to produce short, high frequency, high peak power rf pulses). Also, higher peak power and gradients are required which impose operational limitations due to breakdown and breakdown related damage, although in general, higher gradients have been achieved at higher frequency. Finally, the transverse wakefields in the structures increase with frequency, making structure alignment tolerances tighter and the required suppression of the long-range wakefield greater. To offset the stronger wakefield effects, beam currents that yield less than optimal rf-to-beam efficiency are typically chosen. Thus, the choice of operating frequency tends to depend on one's perception of affordability and manageable operating conditions.

6.5.2.1.4 General Structure Requirements Having chosen a frequency, there are four general requirements on the accelerator structure design: it must transfer the rf energy to the beam efficiently to keep the machine cost low; it must be optimized to reduce the short-range wakefields which depend on the average iris radius; it must suppress the long-range transverse wakefield to prevent multibunch beam breakup (the resonant amplification of bunch betatron motion by the bunch-to-bunch transverse wakefield coupling); and it must operate reliably at the design gradient. The design choices and R&D related to meeting these requirements are discussed in the sections that follow. In addition, there are sections that address structure fabrication, operating environment, operating experience, and the potential for increasing gradient.

6.5.2.2 Choice of Structure Parameters

For the JLC-X/NLC, the choice of structure parameters was greatly influenced by the trade-off between increasing rf-to-beam energy transfer efficiency and lowering short-range wakefield related emittance growth. The emittance growth is caused by the head-to-tail transverse wakefield deflections generated when the bunches travel off-axis through the structures. Resonant head-to-tail amplification is suppressed by introducing a correlated energy spread along each bunch (called BNS damping). The size of the remaining non-resonant emittance growth depends on a number of factors including the average iris radius, the bunch charge, and the achievable beam-to-structure alignment (the goal is about 10 μm). The average iris radius and the bunch charge also affect the rf-to-beam efficiency: higher efficiency generally comes at the expense of increased emittance growth. As a result of this basic trade-off and cost driven constraints on structure length and peak power, an average iris radius of 18% of the X-band wavelength was chosen for the linac structure design.

Defining the structure parameters required a number of other design choices. A traveling-wave structure was selected because standing-wave designs are generally more expensive. A disk-loaded waveguide geometry was used since disk-shaped cells are easy to manufacture. The iris surface field along the structure was held roughly constant to avoid having one region of the structure limit the gradient because of rf breakdown. The gradient profile was shaped by varying the rf group velocity along the structure, a common method for achieving a constant gradient. The initial choice for the phase advance per cell was 120°, the same as for the SLAC S-band structure. This value yields a high shunt impedance per unit length. The choice of both the structure filling time and rf pulse length were strongly influenced by the rf attenuation time in the structure (about 100 ns), which varies weakly with group velocity. That is, nearly optimal rf-to-beam efficiencies can be achieved with filling times equal to the attenuation time for low beam loading, and the rf pulse length needs to be significantly greater than the filling time, but not too large or it becomes more economical to increase the machine repetition rate rather than the pulse length.

The choices in these respects constrained the basic structure geometry, and resulted in a 206-cell, 1.8-m long structure with a group velocity varying from about 12% to 3% c. The initial choice of a 70 MV/m unloaded gradient (G_U) is close to optimal in the tradeoff between energy-related costs (*e.g.*, modulators and klystrons), which scale roughly

as G_U, and length-related costs (*e.g.*, structures and beam-line tunnel), which scale roughly as $1/G_U$. However, once high gradient testing of such structures began in earnest, it became clear that they would not reliably operate at this gradient due to breakdown limitations.

This discovery prompted an aggressive program to develop higher gradient structures (see Section 6.5.2.6). The results from this program have led to the adoption of a lower group velocity (5.1% c to 1.6% c) structure design for the JLC-X/NLC main linacs. This structure is shorter (0.9 m versus 1.8 m), has a longer filling time (120 ns versus 104 ns) and has a somewhat lower shunt impedance (81 Mohm/m versus 89 Mohm/m) than the 1.8 m design.

The rf-to-beam efficiency achievable in a structure depends on the choice of beam current and bunch train length in addition to the structure parameters. In the present JLC-X/NLC configuration, a 0.86 A, 269 ns long bunch train is accelerated during each pulse. This requires an rf pulse length of 400 ns including rise time, so the fill-time efficiency (bunch train length divided by rf pulse length) is 67%. The beam current produces 23% beam loading relative to the 65 MV/m unloaded gradient, and results in a steady-state rf-to-beam efficiency of 53%. Thus, the overall efficiency is 36 %, ignoring energy overhead. A higher efficiency could be achieved by increasing the beam loading, but the wakefields would be unacceptably large, the loaded accelerating gradient would be reduced, and the linac would have to be longer.

From the fundamental rf frequency point of view, the JLC-C structures follow the same design criteria. They exhibit comparable parameters: length 1.8 m, phase advance $3\pi/4$ per cell, iris radius ranging from 0.171–0.126 λ, group velocity from 11.4% c to 3.6% c.

The present CLIC parameters are based on the Tapered Damped Structure (TDS) design. The design criteria for the TDS included requirements on short and long range wakefields and optimization of the shunt impedance. The average iris radius to wavelength ratio (a/λ) was chosen to be 0.2. This is a compromise between low short-range wakefields, favoring large a/λ, and the desire for high shunt impedance, favoring small a/λ. A cell design with 0.55 mm thick irises and a $2\pi/3$ phase advance was also chosen to maximize shunt impedance.

However, recent observations of field limitations due to electrical breakdown and related surface damage in 30 GHz prototype structures have shown that the present TDS design will not meet the gradient requirements for CLIC without modifications to its geometry. A weak point of the TDS design is the excessive pulsed surface heating in the vicinity of damping waveguide entrances. A program of structure development and high power testing using different structure geometries and materials is under way, accompanied by theoretical studies of wakefield control. The goal is to produce a new design meeting the gradient, pulse length and wakefield requirements of CLIC. The directions being taken in this process are discussed in Section 6.5.2.3 and Section 6.5.2.6.

6.5.2.3 Wakefield Suppression

Once the basic structure design had been selected, a method for suppressing the long-range transverse wakefield was needed. The long-range wakefields are generated as the beams traverse the accelerator structures, and if not suppressed, would produce an enormous amplification of any betatron motion of the bunch train. Several techniques to reduce these wakefields have been developed and are described here. For the JLC-X/NLC and CLIC, the

techniques were developed for their initial structure designs and are described in this context.

For the JLC-X/NLC, the transverse wakefield must be reduced by about two orders of magnitude during the 1.4 ns between bunches. To achieve this difficult goal, a combination of cell detuning and damping was chosen. For the detuning, each cell of the structure is made to have a slightly different dipole frequency so that the wakefields destructively add by the time the next bunch arrives. The frequency variation is chosen to produce a Gaussian-like distribution in the product of the dipole mode density and the dipole mode coupling strength to the beam. This detuning produces an approximately Gaussian falloff in the net wakefield generated by each bunch, and works well to suppress the wakefield for about 30 ns, after which the amplitude increases due to a partial recoherence of the mode excitations. To offset this rise, weak mode damping was introduced by coupling each cell through longitudinal slots to four TE_{11} circular waveguides (manifolds) that run parallel to the structure. This reduces the dipole mode quality (Q) factors from about 6000 to 1000, limited by the propagation time of the dipole-mode energy through the cells.

Successful implementation of the damping and detuning required major advances on two fronts. One was the accurate modelling of wakefield generation in structures whose geometry varies from cell to cell. This was achieved using an equivalent circuit model where the circuit parameters were obtained via 3-dimensional finite-element calculations of a subset of cells. Another key advance was in the precision machining of the cell shapes to produce the desired acceleration and dipole mode frequencies.

The wakefields of three damped and detuned, 1.8 m structures have been measured to date. Although the wakefields for all three structures were larger than acceptable for the JLC-X/NLC, the suppression was within factors of 2–5 of the two-orders of magnitude reduction required. In two cases, there were known errors during the structure fabrication, which when simulated in the structure model, yielded wakefields in good agreement with the measurements. In the third case, good agreement was achieved after including 12 MHz rms, random cell-to-cell frequency errors in the model, which were larger than the 5 MHz rms errors expected from a limited set of cell measurements made prior to assembly. These comparisons have lent confidence that the wakefields can be accurately modelled. Currently, these techniques are being applied to the high gradient structures being developed, with testing expected in summer 2003.

The C-band group structures include an azimuthal choke joint in each cell for wakefield damping. With this geometry, the acceleration-mode fields are confined within the cell volume while the dipole mode fields extend radially beyond the choke area where they are absorbed in a SiC ring. Although this strong-damping scheme is simpler than that of JLC-X/NLC, the addition of the choke joint reduces the acceleration mode shunt impedance by about 20%.

A full length (1.8 m) "choke-mode" structure was built and its wakefield measured. The results showed that the dipole modes Q's were reduced below 20 as desired. However, a trapped mode in a higher band made the net wakefield higher than acceptable after 1.6 ns. The origin of the trapped mode was subsequently discovered, and corrections will be made in future designs so that it is heavily damped.

For the CLIC TDS design, the long-range wakefield must also be reduced by a factor of about 100 between bunches (0.7 ns). The approach chosen to achieve this uses a

combination of detuning and strong, local damping. The damping is realized by four transverse waveguides coupled to each cell, each terminated by a SiC load, arranged in a "flying chimney" configuration. The acceleration mode is below cutoff in these waveguides, but like the C-band choke joints, they produce a moderate loss (20%) in the acceleration mode shunt impedance.

To test this scheme, a 15 GHz scaled version was built so the larger iris radii would allow wakefield measurements in the ASSET facility at SLAC. A two-orders of magnitude wakefield reduction was observed by 1.4 ns, the equivalent bunch spacing at 15 GHz. However, a low frequency trapped mode in the beam pipe to vacuum vessel interface region produced a wakefield that dominated at longer times. This mode can be easily eliminated in future designs.

As noted previously, the pulse surface heating near the waveguide entrances in the TDS cells is large (250°C at the design gradient of 150 MV/m). Changes to the cell and waveguide geometry are being studied to reduce the pulse heating. Another damping approach being developed uses radially slotted irises to transport the dipole mode energy outside the cell. The geometry reduces pulse heating because of the small slot sizes. To test this concept, a short 3 GHz structure with slotted irises has been fabricated and high-power tested up to a 25 MV/m average accelerating field with 1.5 μs pulses. No degradation in performance was seen due to the slots.

6.5.2.4 Fabrication

6.5.2.4.1 JLC-X/NLC Over the past decade, manufacturing processes for X-band cells and structures have been developed by a SLAC-KEK collaboration, with participation by Lawrence Livermore National Laboratory and the involvement of several precision machining companies. In addition, the JLC group at KEK, in Japan, has made good progress toward developing industrial partnerships for fabricating cells and assembling structures.

The process developed for building the 1.8-m structures begins with the rough machining of high-purity copper disks using conventional lathes and mills. Rough machining leaves more than 40 μm of extra copper on all surfaces except for the coupling slots and manifolds. Follow-up precision turning, performed using single-crystal diamond tools, yields μm level accuracy and 50-nm (rms) surface finish. As the diamond turning is completed, microwave quality-control measurements are made of the acceleration and dipole-mode frequencies of each disk. If a systematic shift of the acceleration frequency is found in a series of consecutive disks, then adjustments are made to the nominal dimensions of the subsequent cells to offset the net phase-advance error. This feedforward correction procedure yields structures with a net phase advance within a few degrees of the design value. The dipole-mode frequencies are checked to eliminate cells with values significantly different (by a few MHz) from those of neighboring cells.

After cleaning and rinsing with ozonized water, the cells are stacked in a special V-block fixture and bonded together by a two-step diffusion bonding process: first at 180°C and then at 890°C. The complete structure is then assembled with flanges, vacuum ports, WR90 waveguides for the acceleration mode, and WR62 waveguides for the dipole modes. It is then brazed in a hydrogen furnace at 1020°C. After a vacuum bake-out, the structure

is installed on a strongback for final mechanical measurement and straightening guided by data from a Coordinate Measuring Machine. This procedure has yielded 1.8-m structures meeting the JLC-X/NLC straightness requirement of 10 μm rms.

A diffusion bonding technique has been adopted for assembling the main body of the JLC/NLC X-band accelerator structures mainly because of its ability to maintain excellent disk-to-disk tolerance during the processing, as well as mechanical sturdiness and good vacuum sealing capability. The initial consideration was that for diffusion bonding to produce acceptable bonding quality, the use of diamond-turned surfaces is of critical importance. However, recent experiences in building accelerator structures for high-power testing indicate that disks that are conventionally machined with poly-crystal cutting tools also exhibit good results in the diffusion bonding processes.

The choice of the cutting tools for the precision machining of X-band accelerator structures (*i.e.*, diamond versus poly-crystal) is another open issue. From the standpoint of controlling the resonant frequencies of individual disks, diamond-turned disks can be fabricated so as to make the post-assembly frequency tuning unnecessary. However, structures made with conventionally machined disks can be also tuned relatively easily via bead-pull measurements. Studies of the relative merits of these two approaches are needed to help the JLC-X/NLC group form the best strategies for mass-producing satisfactory accelerator structures in a cost-effective manner.

The structure manufacturing efforts will grow in the future with the increasing involvement by Fermilab, which joined the NLC collaboration in 1999. Working with off-site fabrication shops, the NLC group there has thus far built three, 20 cm X-band structures. In the next year, they plan to produce at least 5.4 m of low group velocity structures for the 8-Pack rf-system demonstration at the NLCTA. The group's long-term goal is to develop the industrial partnerships needed to manufacture the full complement of X-band structures for NLC.

6.5.2.4.2 CLIC So far nine 30 GHz prototype structures (without HOM damping) have been built and high power tested. These prototypes were of the constant impedance type. Eight of the structures were fabricated from 86 OFHC copper disks using single-point diamond turning and were assembled using a specially developed CLIC brazing and diffusion bonding technique at 820°C. This assembly technique results in fundamental-mode Q values close to the theoretical values (∼99%). In contrast to JLC-X/NLC structure fabrication, all brazing operations are done in vacuum instead of hydrogen. The CLIC team has not had any temperature control problems and wants to avoid diffusing hydrogen into the copper.

The cells for all structures have been machined by European industry. The ± 2 μm machining tolerances imposed by long range wakefield constraints were in all cases met. All but one of these structures were assembled and brazed at CERN (one was assembled and brazed by industry). Seven of the eight structures had single-feed, conventional couplers which produced a very asymmetric field in the first cell of the structure, and created a very high ratio of peak surface field to accelerating field.

A study of the mass-production cost of the precision machining of these copper disks was made by four independent firms in 1993. The four estimates were very close and showed

that the cost was very reasonable. An equivalent study for structure assembly and brazing has not yet been made.

The ninth structure that was built is very different. It was made by clamping tungsten irises and copper disks together, and was mounted and tested in a vacuum can. Its couplers are of the single-feed mode-launcher type and were also clamped onto the structure. These couplers produce a very symmetric field in the first cell of the structure, with peak surface fields less than those in the other cells. The clamping and vacuum-can technique was first used by the CLIC team for the TDS wakefield measurements described earlier.

6.5.2.5 Structure Environment

The accelerator structure dimensions must be kept stable as rf power and beam current are varied. For the normal-conducting designs, it is not necessary to actively tune the structures by mechanical means. However, the average temperature needs to be controlled to about 0.5°C to prevent significant changes in the bunch energy and energy spread. Such tolerances have been easily met in a wide variety of linac systems.

The JLC-X/NLC designers are evaluating a less costly cooling scheme compared to that in the SLAC linac and NLCTA. It would use a relatively low flow of water, about a third of that nominally used, to cool the several kilowatts of power dissipated per meter of structure. In this case, the structure temperature rise during operation is estimated to be about 10°C. It is expected that temperature stability requirements can be met but further engineering is required to determine the minimum cost design.

6.5.2.6 High Gradient Development

6.5.2.6.1 High Gradient Structure Development for JLC-X/NLC High-power testing of NLC and JLC prototype structures began in earnest in 1999 with the improvements to the high power testing capability at the NLC Test Accelerator (NLCTA). The difficultly encountered in processing one of the 1.8-m structures to 70 MV/m with 240 ns pulses led to the discovery that breakdown-related damage was producing a significant alteration in the rf properties of the structure at gradients less than 70 MV/m. The damage was manifested as an increase in the rf phase advance through the structure and was associated with severe pitting of the cell irises. Phase advance measurements of several other 1.8-m structures showed that the damage had begun at unloaded gradients above 45–50 MV/m. A revealing observation was that the damage was much more pronounced in the upstream ends of the structures where the rf group velocity is greatest. Such a dependence on group velocity may be due to the higher rf power required to achieve a given gradient at higher group velocity.

Besides the phase shifts, the breakdown rate in the 1.8 m structures remained high at gradients above 60 MV/m, indicating the damage was likely continuing. Thus, the effective gradient would eventually diminish due to out-of-phase acceleration. The phase change rate was estimated to be about 20° per 1000 hours of operation at a 60–70 MV/m gradient, which would make the structures ineffective in a few months. While ideally no phase change would occur during operation, a shift up to 0.5° per 1000 hours would likely be acceptable. This would result in only a 5% loss of effective gradient in 20 years of operation in a worst case scenario where no effort is made to compensate for the phase change (*e.g.*, increasing the structure operating temperature).

In operational terms, an acceptable breakdown rate depends on (1) the number of structures turned off after a breakdown, (2) the recovery time needed to bring the structures back to full power and (3) the fraction of structures allocated for spares. For the JLC-X/NLC, six structures (one girder's worth) will be turned off after a breakdown in any of the structures, the recovery time will be 10 seconds, which has been tested, and 2% of the structures (19 girders per linac) will be used as "hot-swappable" spares. Given these values, a structure breakdown rate of 1 per 3 hours at the 120 Hz repetition rate would essentially never deplete the structure reserves (this would occur about once per year and would take less than 10 seconds to recover from). At this rate, approximately one structure in each linac would breakdown every 100 pulses, yielding at most a 0.02% change in the beam energy during that pulse. The beam energy would fluctuate by >0.1% only once a year due to multiple structure breakdowns per pulse (the Final Focus bandwidth is ±0.5% in comparison).

To address the structure damage problem, a program was launched in spring 2000 to develop lower group-velocity structures. Much progress has been made since then toward understanding high gradient performance. The advances have resulted from an aggressive experimental program, which has included tests of three pairs of low group velocity traveling-wave structures ('T' series,with different lengths, 20, 53 and 105 cm and group velocities, 5% c and 3% c at the upstream ends), an initial test of a pair of high phase advance traveling-wave structures ('H' series), and operation of three pairs of standing-wave structures. In addition, various improvements were made to the structure cleaning, handling and processing procedures to determine their impact on high-gradient performance. A brief summary of the results from these studies follows.

The rf processing of the T-Series structures started at higher gradients (55–65 MV/m) than that (35–45 MV/m) for the 1.8 m structures. In addition, much less damage was observed in these structures at gradients above 70 MV/m than in the 1.8 m structures at gradients of 50–65 MV/m. After processing to 80–85 MV/m, the breakdown rate at 70 MV/m was dominated by events in the input and output couplers. The breakdown rates in the body of the structures (*i.e.*, excluding the couplers) at 70 MV/m were close to acceptable for the JLC-X/NLC at the design pulse width of 400 ns. For the three 53 cm, 3% c initial group velocity structures that were tested, the breakdown rates were <0.1, 0.2, and 0.3 per hour, respectively, while the goal is <0.1 per hour given the structure length and NLCTA repetition rate of 60 Hz.

An autopsy of the input coupler of one of the structures revealed melting on the edges of the waveguide openings to the cell, and extensive pitting near these edges and on the coupler iris. The waveguide edges see large rf currents that are a strong function of their sharpness, and the associated pulse heating can be significant. By design, the edges in the T-Series structures were sharper (76-μm radius) than those in the 1.8-m structures (500-μm radius). Recent calculations have shown that the pulse heating for the T-Series structures is in the 130–270°C range, well below the copper melting point, but high enough to produce stress-induced cracking, which can enhance heating.

Based on these observations, a 53 cm, 3% c structure was built with couplers designed to have much lower pulse heating. This structure is currently being tested and has performed very well, with no obvious enhancement of the coupler breakdown rates relative to the other cells. For the full structure, a breakdown rate of about 1 per 25 hours has been measured at 73 MV/m with 400 ns pulses, and after further processing to 92 MV/m, a similar rate has

been measured at 90 MV/m. All future structures will be made with couplers similar to those used in this test.

Although the results from the T-Series structures are very encouraging, their average cell iris radii are too small to meet JLC-X/NLC short-range wakefield requirements. To increase the iris size while maintaining a low group velocity, a structure design with thicker irises and a higher phase advance per cell (150° instead of 120°) design has been adopted. Two such structures (H-Series) have been built, one 60 cm long with an initial group velocity of 3% c, and the other 90 cm long with an initial group velocity of 5% c. Both are detuned for wakefield suppression, but do not include manifolds for wakefield damping.

Unfortunately, these structures have the earlier, T-Series type couplers since they were built before the coupler pulse heating problem was discovered. Making the problem worse, the H-Series structures have lower shunt impedance than the T-Series structures, so the pulse heating is relatively high. During their processing at NLCTA, the coupler breakdowns have indeed limited the gradient to values lower than that achieved with the T-Series structures. In addition, at short pulse lengths where the coupler events did not dominate, the processing rate was much slower than that for the T-Series structures. The larger iris thicknesses of the H-Series structures are certainly a contributing factor, but they do not explain the full difference.

The best results to date have been achieved with the 60 cm, 3% c structure, which has been processed to 72 MV/m with 400 ns pulses. At 65 MV/m, the current JLC-X/NLC design gradient, the breakdown rate in the body of this structure meets the goal of <1 per 10 hours while the input coupler breakdown rate is about 25 per hour. The program until summer 2003 is to test several H-Series structures with improved couplers, culminating in one that is fully damped and detuned for wakefield suppression. By the end of 2003, 5.4 m of such structures (with and without damping) will be powered with the 8-Pack rf source to demonstrate full system integration and to improve performance statistics.

Another approach being explored for achieving higher gradients is to use short standing wave structures that require much lower peak power than the traveling wave structures. The standing wave structures tested so far are 20 cm long, contain 15 cells and have a beta coupling of one or two. They are operated in pairs, which allows the power reflected from them during their approximately 100 ns fill/discharge periods to be routed to loads.

Three such pairs have been tested during the past year. However, only one pair performed well at the flattop pulse width of 270 ns and earlier JLC-X/NLC loaded gradient requirement of 55 MV/m (unlike the traveling-wave structures, the standing wave structures do not need to operate above the JLC-X/NLC loaded gradient). After processing, the average breakdown rate for this pair at 55 MV/m was about 0.1 per hour per structure during a several hundred hour period, which is about a factor of 2 higher than desired for these short structures. Also, no discernable shift in frequency (<100 kHz) was measured in either structure after 600 hours of operation. The other pairs showed higher breakdown rates (>1 per hour) at 55 MV/m and one pair showed frequency shifts of several hundred kHz.

From rf and optical measurements made during operation and after removal from NLCTA, it appears that most of the breakdowns occurred in the coupler cells of the standing wave structures. The structure performance roughly correlates with the predicted temperature rises on the input waveguide edges in the coupler cells. That is, for JLC-X/NLC running

conditions, the temperature rise for the best performing pair was 40°C, while that for the other two pairs was 60°C and 150°C. For the next pair of structures to be tested, a coupler with a lower temperature rise (<20°C) will be used, and choke-mode cells will be included to test their high gradient properties in preparation for their use to damp wakefields.

6.5.2.6.2 Basic Studies at NLC on the Physics of RF Breakdown As a complement to the structure testing, the NLC group is committed to a strong program of theoretical studies, computer simulations and experimental measurements directed toward understanding the underlying physics of rf breakdown. A simple theory indicates, for example, that extensive surface damage may occur when an area on the surface is brought to the melting point by electron bombardment before the end of the rf pulse. This points the way toward the use of other materials, such as stainless steel, tungsten or molybdenum as materials for the iris tips in a copper structure (see CLIC results below). Computer simulations, using an advanced 3D particle tracking code, are used to follow the motion of electrons and ions emitted from small areas of plasma formed near field emission sites, and to calculate the power density and resulting temperature rise at areas where the electrons impact on the surface.

A comparison of the results from theory and simulations with experiment is best carried out by high-field tests on simple structures. A well-instrumented test bed has been set up for measurements on short sections of rectangular waveguide with enhanced surface fields, and on short sections of traveling-wave (TW) and standing-wave (SW) structures. So far, waveguide sections having different group velocities and made from different wall materials have been tested. These measurements have provided experimental verification that, compared to copper, significantly higher fields can be sustained on a stainless steel surface without breakdown. A series of tests is now in progress in which a short length of accelerator structure, consisting of two standard structure body cells and two coupling cells, is placed between two low-field mode launcher-type couplers. Because these test sections do not include couplers and are demountable, they can be cycled through the test setup rapidly, compared to the time required to build and test a full structure with couplers. The dependence of processing time, breakdown rate and limiting gradient on a number of structure variables can be studied. Some tests in progress or planned are: the dependence of the preceding breakdown-related parameters on group velocity for TW structures; a comparison of breakdown parameters for TW structures versus SW structures for a given iris aperture; the dependence on iris tip material; the dependence on fabrication variables related to machining and surface preparation; and a measurement of potential surface damage near coupling apertures in structure cells with damping.

6.5.2.6.3 High Gradient Structure Development at CLIC The CLIC group ran a program of 30 GHz high-power structure testing using CTF2 as the power source. CTF2 provided 30 GHz rf pulses of up to 280 MW with a variable pulse length from 3 to 15 ns. This pulse length was larger than the filltime of the structures built so far, but short compared to the nominal 130 ns pulse-length of CLIC. The probe beam of CTF2, with its two magnetic spectrometers, allowed a precise beam-based measurement of the average accelerating gradient in the structures. This was a very useful cross-check of the gradient derived from the 30 GHz power measurements. Since the available power by far exceeded the power needed for structure testing, a simple pulse-stretcher was installed to increase the

pulse length to 30 ns. Unfortunately, CTF2 was closed down and dismantled at the end of 2002 to make way for a new CLIC test facility, CTF3. This new facility will produce 30 GHz rf power pulses of the nominal 130 ns length. High-gradient testing with this new source is expected to start in spring 2004. In another structure-related activity, the CLIC team is collaborating with JINR/Dubna to carry out pulsed-surface-heating tests of copper cavities using their 30 GHz FEL as the power source. These tests will assess the fatigue properties of copper, and other materials may be studied as well.

In 1994, a small aperture (6 mm), low group velocity, 26-cell X-band structure was built with CLIC technology and tested at SLAC. It achieved a peak accelerating gradient of 150 MV/m with a 150 ns pulse (the average gradient was 125 MV/m) without damage, demonstrating the technical feasibility of producing 150 MV/m gradients with copper structures.

The constant impedance copper structures tested before 2002 in CTF2 reached mean accelerating gradients of only 60 MV/m (confirmed by both beam acceleration and rf power measurements). At this field level, considerable surface damage was observed on the first iris which connects the input coupler cell to the first regular cell. No significant damage was seen in the downstream cells. This is easily understandable because the coupler cell has the highest surface field in the structure (the surface field corresponding to a 60 MV/m mean acceleration is 264 MV/m, a ratio of 4.4). The damage pattern resembles the field distribution pattern which suggests a correlation between peak surface field and damage. RF conditioning to the level where damage occurs took typically 3×10^5 rf pulses. In a recent experiment (June 2001), the damaged copper iris was replaced by an iris made of tungsten. In this configuration the structure reached 72 MV/m accelerating field. The corresponding surface field on the tungsten iris is 317 MV/m. Although the structure was powered for 5×10^5 pulses to the same field levels, the tungsten iris was undamaged. When the tungsten iris was replaced by a copper iris and the pulse length was shortened to 3 ns, a record peak accelerating gradient of 160 MV/m was obtained with 5×10^5 pulses. Although the pulse energy was the same as in the 72 MV/m run at 15 ns, no damage occurred.

During 2002, three structures made from either a different material, with a reduced E_{surf}/E_{acc} ratio along the structure were tested at high power in CTF2, or both. The geometry of the structures was deliberately kept simple for these tests with no complicating features such as damping waveguides so that the basic underlying limitations could be clearly observed. The first structure tested had an a/λ of 0.175 with a $2\pi/3$ phase advance, a E_{surf}/E_{acc}=2.2 and v_g=0.046 c. The couplers were of the mode-launcher type. The surface field in the coupler nowhere exceeded the field in the regular cells. All irises were made of tungsten with copper rings clamped between them (see paragraph on structure fabrication). The second structure had the same cell geometry, but was made entirely from OFHC copper and assembled by a braze/diffusion bond at 820°C in vacuum. The third structure had all irises made from molybdenum with copper rings clamped between them.

The first structure, with tungsten irises, was conditioned (15 ns at 5 Hz) to an average accelerating gradient of 125 MV/m, with a peak accelerating field in the first cell of 152 MV/m and a peak surface field of 340 MV/m. When the inside of the structure was examined with an endoscope, there was no observable damage along the body of the structure, and in particular none in the coupler. The second structure, entirely made from copper, reached an average accelerating field of 102 MV/m with a peak accelerating field in the first cell of 114 MV/m and a peak surface field of 255 MV/m. Contrary to the

tungsten-iris structure, the copper structure showed signs of surface damage on the first regular iris, where the surface E-field is highest. The third structure, with molybdenum irises, was conditioned to an average accelerating gradient of 150 MV/m, with a peak accelerating field in the first cell of 193 MV/m and a peak surface field of 432 MV/m. No damage was observed. From these results and past CTF2 results, it is inferred that tungsten and molybdenum can support considerably higher surface fields before breakdown damage occurs, while copper shows surface damage for surface fields exceeding 250 MV/m. This damage inhibits rf conditioning of copper surfaces beyond this level. The same copper structure was tested with a 30 ns pulse length using an rf pulse stretcher in CTF2. The same accelerating gradient was obtained as with 15 ns pulses. This result gives a first indication that the dependence of breakdown level on pulse length is weak if the pulse length is larger than the time needed to develop a full breakdown (typically 10 ns), but small compared to the pulse length for which surface heating becomes important. The achievable rf power level with the CTF2 pulse stretcher was insufficient to drive the tungsten and molybdenum structures to their breakdown points. More tests are needed to evaluate more precisely the dependence of breakdown damage for these materials on pulse length.

A second tungsten-iris structure will be built with a $\pi/2$ phase advance and with an a/λ=0.2, E_{surf}/E_{acc}=2 and v_g=0.083 c. A comparison of the gradients achieved with the two tungsten-iris structures will hopefully enable the effects due to surface field and group velocity to be distinguished.

The lower conductivity of tungsten reduces the Q value relative to copper. For the structure already tested, the Q value is 33% lower. This Q change reduces the rf-to-beam efficiency by approximately 20%. If tungsten is only used in the regions of the cells where the surface electric field is more than 50% of the peak surface field, then the Q would only be reduced by 5%, and the rf-to-beam efficiency by 1%. Studies of the technical feasibility for such a configuration have just started.

A series of tests performed with single cell copper cavities at 21 GHz, 30 GHz, and 39 GHz showed no significant dependence of the breakdown limit on frequency. All these cavities reached peak surface fields around 350 MV/m. Other frequencies could also be created in CTF3 in order to evaluate more precisely the much discussed behavior of rf structures versus frequency. This would be a good opportunity for a global collaboration between laboratories.

6.5.2.6.4 Basic Studies at CLIC on the Physics of RF Breakdown The CLIC team has undertaken a vigorous program of theoretical studies, computer simulations and experimental tests aimed at understanding the underlying physics of rf breakdown. There is evidence to suggest that the melting point of the material used and possibly its vapor pressure may play an important role in determining achievable gradients, and the use of other materials such as tungsten or molybdenum for the iris tips in copper structures is being pioneered.

6.5.2.6.5 High Gradient Structure Development for JLC-C The C-band groups at KEK and RIKEN are planning to conduct their first systematic high-power tests of 1.8 m, choke-mode structures at an unloaded gradient of 42 MV/m during 2003. They are

encouraged by a 1994 high power test of a short, low group velocity (0.8% c), choke-mode, S-band structure, which processed to 50 MV/m.

6.5.2.7 Operational Experience

The bulk of operational experience with X-band structures has come from the NLC Test Accelerator (NLCTA) at SLAC. This facility, which was commissioned in 1996, is a test-bed for X-band accelerator systems. The power sources (XL4 klystrons and SLED-II pulse compressors) have operated reliably, energizing 12 X-band accelerator structures for an integrated total of about 10,000 hours. The NLCTA has accelerated high-quality pulse trains with energy spread within the JLC-X/NLC specification of 0.3%.

The new generation of improved X-band components will be added to the NLCTA over the next two years for a demonstration of the proposed JLC-X/NLC rf system. The components include 11 m of high-gradient accelerator, a multimode SLED II pulse compression system, eight 75-MW klystrons with periodic permanent-magnet focusing, and a solid state, high-voltage pulse modulator.

Operational experience for CLIC structures comes from CTF2. In 1999, a string of five structures was installed in the CTF2 probe beamline and operated for approximately 200 hours at an average gradient of 40 MV/m. The 30 GHz rf power was delivered by 4 power extraction structures installed on the CTF2 drive beam, running parallel to the probe beamline. This CTF2 run gave valuable experience on setup procedures for two beam accelerators. In 2000, CTF2 was converted in a 30 GHz high power test stand allowing testing of only one structure at a time, but at much higher power levels.

6.5.2.8 Potential for Upgrading to Higher Gradients

The scaling of the breakdown-limited gradient with rf frequency has been the subject of both theoretical and experimental investigation for many years. More recently, it has been realized that pulse length plays an important role. Currently, the role that structure geometry (group velocity, standing wave versus traveling wave) and structure material (*e.g.*, tungsten iris tips) plays in determining the breakdown gradient is also being investigated. But it is fair to say that a comprehensive theory of rf breakdown is still some distance in the future, and that we are currently taking a mainly phenomenological approach to the problem (try lots of things and see what works), with some guidance from a few simple theoretical ideas.

From their experiments, Loew and Wang [33] concluded that, at roughly constant pulse length, the breakdown-limited gradient scales approximately as the square root of frequency. Their scaling expression gives a peak surface field of 660 MV/m at 11.4 GHz. A peak surface field of this order at a pulse length of several microseconds was actually reached on the reentrant nose cone of a cavity in the "Windowtron" test stand at SLAC [34]. In addition, we note that the capture threshold for dark current scales linearly with frequency (the threshold is 61 MV/m at 11.4 GHz). These factors encouraged the NLC to continue to focus on the linear collider design effort at X-band, in spite of difficulties associated with a higher frequency, such as tolerances and rf power production.

It was seen in Section 6.5.2.6 that the gradient design goal for the JLC-X/NLC is close to being met. There are prospects for increasing the gradient well beyond the JLC-X/NLC

design goal. In experiments in which breakdown is studied in a short low group velocity section of waveguide made of different materials (see Section 6.5.2.6.2), Tantawi and Dolgashev [35] found that the breakdown field is 20–30% higher for stainless steel compared to copper. This higher gradient could be used either to increase the operational safety margin or to increase the machine energy.

As was also mentioned in Section 6.5.2.6, a gradient of 150 MV/m at a 15 ns pulse length has recently been reached in experiments at CLIC using tungsten irises. It remains to be seen whether this success can be extended to reach the unloaded design gradient of 172 MV/m at 130 ns. In any case, CLIC is not looking beyond the design gradient because pulse surface heating and drive beam energy requirements would pose other serious limitations that seem difficult to overcome in the present CLIC scheme.

The JLC C-band strategy is also not aiming beyond the unloaded design gradient of 42 MV/m. They would add a length of X-band linac to upgrade in energy.

6.5.3 Accelerator Structures: Conclusions

6.5.3.1 Introduction

The choices that were made for operating frequency and technology by all linear collider groups were closely tied to specific performance expectations for the accelerator structures. In particular, all designs assumed that stable operation could be achieved at gradients higher than had been previously demonstrated in comparable structures, and that the long-range wakefields generated in the structures could be suppressed to a level that would keep multiple bunch emittance growth within acceptable limits. Meeting these goals has been the major R&D focus by these groups. The choices made for operating frequency and technology have also had a strong influence on other structure-related issues, such as alignment requirements and ease of fabrication and operation.

An important parameter for any linear collider is the efficiency for the conversion of rf power to beam power. The structure efficiencies (rf input to beam), when accounting for the structure filling time and energy overhead are, for C-band, JLC-X/NLC, and CLIC, 26%, 27%, and 23% respectively. In general, higher efficiencies (and higher beam currents) have been traded off in these designs to reduce wakefield strength, the number of structures, linac length and peak power requirements. On the plus side, the resulting low beam loading (<26%) has the advantage of easing beam current stability requirements. The TESLA structure efficiency is 59%.

6.5.3.2 High Gradient Structure Development

6.5.3.2.1 Concerns for Achieving TESLA Design Gradient The TESLA group has made significant progress during the past decade in improving the surface processing of niobium, allowing them to achieve gradients exceeding 25 MV/m. Thus far, they have produced about 40 nine-cell cavities that have operated at CW with acceptable power losses at gradients between their 500 GeV c.m. design goal of 23.8 MV/m and 35 MV/m. In addition, an eight-cavity cryomodule has accelerated beam at 22.7 MV/m. This is the highest acceleration achieved so far by a TESLA module. Several more cryomodules are in

the queue and they are expected to exceed this gradient. Although the fault rates and recovery times during such operation are just beginning to be better quantified, down-time statistics recorded at 19–22 MV/m suggest that the cavities could run with acceptable down-times in TESLA, at least at these lower gradients. While these results are encouraging, the cavities will likely have to be capable of operating at 35 MV/m initially if the upgrade goal to 800 GeV c.m. is to be considered seriously. The use of an electropolishing technique for etching the cavity surfaces has yielded about 15 single-cell cavities that meet the upgrade requirements. Recently, three nine-cell cavities have also met these criteria during CW operation. During the next year, one of the TESLA group's goals is to build an eight-cavity cryomodule that will accelerate beam at 35 MV/m.

In addition, the long-term behavior of the high power couplers needs to be evaluated further.

R&D (Ranking 2):

- Long term testing of several cryomodules at design gradient (23.8 MV/m) with acceptable quench behavior and coupler performance.

R&D (Ranking 3):

- Evaluate dark current effects at TTF2.

6.5.3.2.2 Gradient Concerns for Normal Conducting Designs The normal-conducting designs have also aimed for high gradients, encouraged by early tests that showed that gradients greater than 100 MV/m are possible. However, these tests were done with standing-wave or low group velocity structures because of the limited peak power available at that time. The higher group velocity structures that were later chosen by the linear collider groups for lower cost (fewer feeds) and lower wakefields have not performed as well. The approach to high gradients has been essentially empirical, as there is little fundamental understanding of rf breakdown and damage mechanisms.

6.5.3.2.3 Concerns for Achieving JLC-C Gradient The unloaded gradient goal of the C-band group at KEK and RIKEN is 42 MV/m. They are planning to conduct their first high power test of their 3.6% c initial group velocity structure in 2003.

R&D (Ranking 1):

- Test structure design at high gradient during 2003.

6.5.3.2.4 Concerns for Achieving JLC-X/NLC Gradient For the JLC-X/NLC, achieving the unloaded gradient goal (originally 70 MV/m with 400 ns pulses) has also been difficult. The initial structure design, in which the group velocity tapered from 12% c to 3% c, incurred significant breakdown related damage near its upstream end at gradients of 45–50 MV/m. A series of six, 5% c and 3% c initial velocity structures that have since been

tested have proven much more robust. Except in the input and output coupler cells, acceptable breakdown rates have been achieved. The high coupler breakdown rates are thought to be related to pulse heating or single-surface multipactoring at the waveguide openings. Recently, a 3% c initial group velocity structure with lower peak magnetic fields in the coupler cells was tested. It achieved acceptable breakdown rates with 400 ns pulses at 73 MV/m, well above the current design gradient of 65 MV/m. However, all of these low group velocity structures have smaller than acceptable iris sizes for the JLC-X/NLC and do not include long-range wakefield suppression. To increase the iris radius while maintaining the low group velocity, a high phase advance (150°) design has been adopted. Testing of a series of such structures has begun. Structures including full wakefield suppression will be tested by summer 2003; this testing is expected to yield an "JLC-X/NLC-ready" design.

R&D (Ranking 1):

- Validate performance of high phase advance, low group velocity structures.
- Choose coupler design and incorporate manifold damping to produce an JLC-X/NLC-ready structure in summer 2003.

R&D (Ranking 4):

- Continue development of standing-wave structure.

6.5.3.2.5 Concerns for Achieving CLIC Gradient The CLIC goal of an unloaded gradient of 172 MV/m in 30 GHz structures is probably the most challenging. Thus far, a gradient of 193 MV/m has been achieved at the upstream end of a short, 5% c group velocity, constant impedance structure made with molybdenum irises. However, due to the power source, the rf pulse length was limited to 15 ns, which is considerably shorter than the 130 ns required. High power testing at 30 ns pulse length has shown similar results. Further high power testing at 30 GHz will be on hold until spring 2004 when a new long pulse power source (CTF3, pulse length variable from 40–500 ns) will start operation.

R&D (Ranking 1):

- Test structures at design gradient and 130 ns pulse length in 2004.
- High power tests of structures with proper wakefield damping.

R&D (Ranking 2):

- Additional tests with tungsten and other iris materials.

6.5.3.3 Basic Studies on the Physics of Surfaces and Breakdown

A program of basic physics studies on gradient limitations is being carried out for both the normal conducting and superconducting projects, in parallel with the effort to develop operationally reliable accelerator structures. For TESLA, these studies include improved understanding of rf surfaces and preparation methods of the surfaces. Another program explores the use of other Type-II superconducting materials. For JLC-X/NLC and CLIC, there is a program of theoretical studies, simulations, and small-scale experiments on breakdown. CLIC is doing pioneering studies on the effect of different iris materials on high gradient performance using a "clamp-together" type structure for fast turnaround. At SLAC, short waveguide sections are being used to explore the effects of different materials. A program using demountable structures with a few cells to explore the effect of different materials, surface preparation procedures and structure geometries is just beginning. At CTF3, one could also test the behavior of structures at different frequencies.

R&D (Ranking 4):

- All projects: strengthen the theoretical studies, simulations and experimental programs aimed at increasing the fundamental understanding of the physics of breakdown in order to achieve higher gradient operation.

6.5.3.4 Wakefield/HOM Suppression

The development of long-range wakefield suppression techniques by all linear collider groups has made considerable progress.

6.5.3.4.1 Concerns for HOM Damping in TESLA For TESLA, the main task is to insure that the dipole modes that couple strongly to the beam are sufficiently damped via HOM couplers at the ends of their cavities. Beam-based measurements of mode properties have shown that this is indeed the case for the strongest bands. However, a trapped mode was found in another band. The HOM couplers have been modified to produce heavier damping of this mode, and will be used in all future cavities. This program is expected to result in satisfactory wakefield suppression.

R&D (Ranking 2):

- Conduct beam test of cavities with modified HOM coupler design starting in 2003.

6.5.3.4.2 Concerns for Wakefield Suppression in Normal-Conducting Machines For the normal-conducting machines, wakefield control has been more of a challenge because of the relatively strong wakefields. These fields need to be reduced by about two-orders of magnitude by the time of the next bunch. The approach has been to use a combination of dipole mode damping and detuning. Different methods have been developed for coupling out the dipole energy for the damping: the C-band group uses so-called choke-mode cells, JLC-X/NLC use distributed coupling to manifolds that run parallel to the structure, and

CLIC uses radial waveguides in each cell. All groups have built test structures whose measured wakefields have come close to meeting design requirements. The reasons for the shortcomings have been identified (*e.g.*, fabrication errors) and are considered correctable.

6.5.3.4.3 Concerns Related to Pulsed Heating A concern related to high power operation is the pulse heating that occurs near the openings of the cells that couple out the dipole energy. The latest design of the CLIC waveguide damped structure has a maximum pulsed temperature rise of 130°C, which is possibly too high. An experimental pulsed surface heating program is underway to determine the acceptable limits for temperature rise. The JLC-X/NLC groups have recently modified the slot shapes in their damped cell design to reduce pulse heating to less than 30°C. Several cells with this new shape will be tested at high gradient by the end of 2002, and complete structures will be tested in spring 2003. The C-band choke mode structure has relatively low pulse heating.

R&D (Ranking 1):

- JLC-X/NLC and CLIC: Incorporate wakefield damping into structure designs without affecting high gradient operation.

6.5.3.5 Tolerances

6.5.3.5.1 Concerns Related to TESLA Structure Alignment Given the low operating frequency of TESLA, wakefield related alignment tolerances for TESLA are relatively loose compared to those for the normal-conducting designs. However, this advantage is partially offset by the difficulty of achieving precise alignment in the cryomodules.

R&D (Ranking 2):

- Demonstrate that multicavity alignment meets requirements.

6.5.3.5.2 Concerns Related to Alignment of Normal-Conducting Structures The smaller size and simpler cooling schemes for normal-conducting structures make them nominally easier to align than the TESLA cryomodules, but the mechanical tolerances are tighter.

R&D (Ranking 3):

- JLC-X/NLC and JLC-C: Demonstrate that the structure alignment meets requirements.

6.5.3.6 Operation and System Tests

R&D (Ranking 2):

- For all designs a test is needed of an rf module, fitted with structures meeting all gradient, wakefield suppression or HOM damping requirements, in an operational setting with beam.

R&D (Ranking 3):

- All designs: Long-term testing of rf modules.

Recommendation: For TESLA, high priority should be given to make TTF2 available for systems tests and high gradient studies in 2003.

6.5.3.7 Structure R&D for Energy Upgrade

TESLA: For the energy upgrade, it is planned to increase the gradient to 35 MV/m. First, it is necessary to show that the gradient is achieved in the standard nine-cells. In a second step the gradient needs to be demonstrated in the 2×9 cell superstructures, if the superstructure is proven to provide sufficient HOM damping. The preliminary results from TTF show that the damping is indeed achieved. As the rf power needed to drive the superstructure is higher than for the standard 9-cells, it needs to be demonstrated that the rf couplers are capable of transmitting the power to the cavity.

R&D (Ranking 1 Upgrade):

- Build an eight cavity cryomodule at 35 MV/m during 2003. Test as soon as possible.
- Evaluate dark current levels and tunnel radiation at 35 MV/m with TTF2.

R&D (Ranking 3 Upgrade):

- Demonstrate superstructures gradient performance, power coupler performance and HOM damping.

JLC-X/NLC: The nominal path for upgrading the JLC-X/NLC energy to 1 TeV is to double the length of the linacs. However, since the SLED-II pulse compression system is capable of providing more peak power by increasing the compression ratio, the possibility also exists for increasing the energy by increasing the gradient. The on-going R&D program of structure development and basic studies of the physics of rf breakdown is directed towards achieving structures which can operate reliably at gradients up to at least 100 MV/m.

R&D (Ranking 4 Upgrade):

- Continue improving structure high gradient performance.

BIBLIOGRAPHY for CHAPTER 6

[1] P. Tenenbaum, P. Emma, L. Keller, Y. Nosochkov, T. O. Raubenheimer and M. Woodley, *Overview of collimation in the Next Linear Collider*, SLAC-PUB-8934. Contributed to IEEE Particle Accelerator Conference (PAC 2001), Chicago, Illinois, 18–22 June 2001.
http://www.slac.stanford.edu/spires/find/hep/www?r=slac-pub-8934

[2] R. Alley *et al.*, *The Stanford Linear Accelerator Polarised Electron Source*, Nucl. Instr. and Meth. **A365**, p.1 (1995), SLAC-PUB-6489 (1994)
http://accelconf.web.cern.ch/AccelConf/p95/ARTICLES/MPE/MPE08.PDF

[3] *Development of a pump-probe facility with sub-picosecond time resolution combining a high-power optical laser and a soft X-ray free electron laser*
http://www-hasylab.desy.de/facility/fel/vuv/projects/pump.htm

[4] E. Bente *et al.*, *The Photoinjector Option for CLIC: Past Experiments and Future Developments*, CLIC note 487, CERN/PS 2001-033 (PP)
http://cern.web.cern.ch/CERN/Divisions/PS/CLIC/Publications/2001.html

[5] I. N. Ross, *Feasibility Study for the CERN CLIC Photo-Injector Laser System*, CLIC Note 462, Central Laser Facility, Rutherford Appleton Laboratory
http://cern.web.cern.ch/CERN/Divisions/PS/CLIC/Publications/2000.html

[6] P. Krejcik, *et al.*, *Recent Improvements in the SLC Positron System Performance*, Proc. 3^{rd} EPAC, Berlin, 1992 (also SLAC-PUB-5786, March 1992)
http://www.slac.stanford.edu/pubs/slacpubs/5750/slac-pub-5786.pdf

[7] V.E. Balakin and A.A. Mikhailichenko, *The Conversion System for Obtaining High Polarized Electrons and Positrons*, Preprint INP 79-85, 1979, and K. Flöttmann, *Investigations Toward the Development of Polarized and Unpolarized High Intensity Positron Sources for Linear Colliders*, DESY-93-161,1993
http://tesla.desy.de/new_pages/TDR_CD/PartII/chapter04/references/Flo93.pdf

[8] L. Rinolfi, *A CLIC Injector complex for the main beams*, CLIC 354.

[9] T. Kamitani, L. Rinolfi, *Positron production at CLIC*, CLIC 465
http://ps-div.web.cern.ch/ps-div/CLIC/Publications/2000.html

[10] *TESLA Technical Design Report*, Part II, chapter 4.3
http://tesla.desy.de/new_pages/TDR_CD/PartII/chapter04/chapter04.pdf

[11] Sheppard, J., Energy Loss and Energy Spread Growth in a Planar Undulator, LCC-086 (2002).

[12] *Linac Coherent Light Source (LCLS) Conceptual Design Report*, Chapter 8, SLAC–R–593, April 2002, UC-414
http://www-ssrl.slac.stanford.edu/lcls/cdr/LCLS_CDR-ch08.pdf

[13] *A Possible Test in the FFTB of Undulator Based Positron Sources*
http://www-project.slac.stanford.edu/lc/local/MAC/MAY2002/MAC_Sheppard.pdf

[14] Ed. K. Floettmann, DESY, Ed. V.V. Paramonov, INR, *Conceptual Design of a Positron Pre-Accelerator for the TESLA Linear Collider*, DESY TESLA-99-14, p.30
http://tesla.desy.de/new_pages/TESLA_Reports/1999/pdf_files/tesla1999-14.pdf

[15] K. Floettmann *et al.*, *Travelling-Wave Positron Injector for TESLA*, DESY TESLA-99-03
http://tesla.desy.de/new_pages/TESLA_Reports/1999/pdf_files/tesla1999-03.pdf

[16] Sheppard, J., Planar Undulator Considerations, LCC-085 (2002).

[17] Sheppard, J., Positron Yield as a Function of Drive Beam Energy for a K=1, Planar Undulator-Based Source, LCC-092 (2002).

[18] W. Kriens, *Basic Timing Requirements for TESLA*, DESY TESLA-01-10
http://tesla.desy.de/new_pages/TESLA_Reports/2001/pdf_files/tesla2001-10-2.pdf

[19] C. Sanelli *et al.*, *Technical Layout of the TESLA Damping Ring*, LNF-01/003 (IR), 2001
http://wwwsis.lnf.infn.it/pub/LNF-01-003(NT).pdf

[20] Y. H. Chin, "Modeling and Design of Klystron," in Proc. of Linac98 (Chicago, IL, USA, 23–28 Aug 1998), p.367.

[21] S. Choroba, "Klystrons for TESLA," presented at LC2002, SLAC, 2002
http://www-conf.slac.stanford.edu/lc02/wg2/WG2_Chroba_Stefan.pdf

[22] A. Buenas and P. Pearce, "A Klystron-Modulator RF Power System for the CLIC Drive-Beam Accelerators," CERN Report, CLIC Note 435, 2000.

[23] H. Matsumoto, T. Shintake, et. al., "Operation of the C-Band 50MW Klystron with Smart Modulator," in Proc. of APAC98 (KEK, Tsukuba, Japan, 23–27 March 1998), p.157.

[24] S. L. Gold, "5045 Klystrons & Thyratron Reliability " presented at LC2002, SLAC, 2002
http://www-conf.slac.stanford.edu/lc02/wg2/WG2_Gold_3602.pdf

[25] R. L. Cassel, J. E. Delamare, M. N. Nguyen, G. C. Pappas, E. Cook, J. Sullivan and C. Brooksby, "The Prototype Solid State Induction Modulator for SLAC NLC," in Proc. of PAC01 (Chicago, IL, USA, 13–22 June 2001), p.3774.

[26] H. Pfeffer, L. Bartelson, K. Bourkland, C. Jensen, Q. Kerns, P. Prieto, G. Saewert, and D. Wolff, "A Long Pulse Modulator for Reduced Size and Cost," Fermilab Report, FERMILAB-Conf-94/182, 1994.

[27] H.-J. Eckoldt, "Pulse Cable for TESLA Modulators," DESY Report, TESLA 2000-35, 2000.

[28] S. N. Simrock, I. Altmann, K. Rehlich and T. Schilcher, "Design of the Digital RF Control System for the TESLA Test Facility," in Proc. of EPAC96 (Sitges, Barcelona, Spain, June 10–13, 1996), p.349.

[29] S. Holmes, C. Ziomek, C. Adolphsen, et. al., "Low-Level RF Signal Processing for the Next Linear Collider Test Accelerator," in Proc. of PAC97 (Vancouver, B.C. Canada, 12–16 May 1997), p.3027.

[30] V. P. Arbet-Engels, C. Benvenuti, S. Calatroni, P. Darriulat, M. A. Peck, A. M. Valente, C. A. Van't Hof. "Superconducting niobium cavities, a case for the film technology," *Nuclear Instr. and Methods, Phys Res, A*: 463 (2001), No. 1–2, pp. 1–8.

[31] Padamsee, Knobloch and Hays, *Rf Superconductivity for Accelerators* (John Wiley, New York, 1998), p. 101–102.

[32] Hassan Padamsee, personal communication.

[33] Gregory A. Loew and J.W. Wang, "RF Breakdown Studies in Room Temperature Electron Linac Structures," SLAC-PUB-4647 (May 1988).

[34] L. Laurent, personal communication.

[35] S. Tantawi, personal communication.